REPORT DOCUMENTATION PAGE

Form Approved OMB NO. 0704-0188

1. REPORT DATE (DD-MM-YYYY)	2. REPORT TYPE	3. DATES COVERED (From - To)
03-08-2015	Final Report	1-Jul-2004 - 28-Sep-2009

4. TITLE AND SUBTITLE
Final Report, "High-Accuracy Near-Surface Large-Eddy Simulation with Planar Topography"

5a. CONTRACT NUMBER
W911NF-04-1-0205

5b. GRANT NUMBER

5c. PROGRAM ELEMENT NUMBER
611102

6. AUTHORS
James G. Brasseur

5d. PROJECT NUMBER

5e. TASK NUMBER

5f. WORK UNIT NUMBER

7. PERFORMING ORGANIZATION NAMES AND ADDRESSES
Pennsylvania State University
Office of Sponsored Programs
110 Technology Center Building
University Park, PA 16802 -7000

8. PERFORMING ORGANIZATION REPORT NUMBER

9. SPONSORING/MONITORING AGENCY NAME(S) AND ADDRESS (ES)
U.S. Army Research Office
P.O. Box 12211
Research Triangle Park, NC 27709-2211

10. SPONSOR/MONITOR'S ACRONYM(S)
ARO

11. SPONSOR/MONITOR'S REPORT NUMBER(S)
44528-EV.11

12. DISTRIBUTION AVAILIBILITY STATEMENT
Approved for Public Release; Distribution Unlimited

13. SUPPLEMENTARY NOTES
The views, opinions and/or findings contained in this report are those of the author(s) and should not contrued as an official Department of the Army position, policy or decision, unless so designated by other documentation.

14. ABSTRACT
Large-eddy simulation (LES) has been plagued by an inability to predict the law-of-the-wall (LOTW) in mean velocity in the surface layer at high Reynolds numbers. Brasseur & Wei developed a theory that explains the source of the difficulty and a framework within which LES can be designed to rectify the problem. The essential difficulty lies in nonphysical frictional content within the discretized dynamical system and the extent to which that frictional content interferes with the inertial scaling that underlies LOTW. Practical models replace inertial flux with dissipative dynamics, so part of this frictional content enters through the subfilter scale (SFS) model. However, this

15. SUBJECT TERMS
large-eddy simulation, LES, overshoot, logarithmic layer mismatch, atmospheric boundary layer, ABL, planetary boundary layer, PBL, turbulent boundary layer

16. SECURITY CLASSIFICATION OF:			17. LIMITATION OF ABSTRACT	15. NUMBER OF PAGES	19a. NAME OF RESPONSIBLE PERSON
a. REPORT	b. ABSTRACT	c. THIS PAGE			James Brasseur
UU	UU	UU	UU		19b. TELEPHONE NUMBER: 814-865-3159

Report Title

Final Report, “High-Accuracy Near-Surface Large-Eddy Simulation with Planar Topography”

ABSTRACT

Large-eddy simulation (LES) has been plagued by an inability to predict the law-of-the-wall (LOTW) in mean velocity in the surface layer at high Reynolds numbers. Brasseur & Wei developed a theory that explains the source of the difficulty and a framework within which LES can be designed to rectify the problem. The essential difficulty lies in nonphysical frictional content within the discretized dynamical system and the extent to which that frictional content interferes with the inertial scaling that underlies LOTW. Practical models replace inertial flux with dissipative dynamics, so part of this frictional content enters through the subfilter-scale (SFS) model. However, this spurious content also enters through the surface stress model, the structure of the grid and dissipation within the numerical algorithm. The research program was directed at discovering the essential nature of the difficulty and specific issues surrounding deviations from LOTW. As a result of a number of key breakthroughs we were successful and were able to propose framework within which LES can be designed to overcome the error. Whereas the essential issues are independent of SFS model, details of the SFS and surface stress models affect the prediction of the von Kármán constant, and likely details of the grid required to capture LOTW with LES.

Enter List of papers submitted or published that acknowledge ARO support from the start of the project to the date of this printing. List the papers, including journal references, in the following categories:

(a) Papers published in peer-reviewed journals (N/A for none)

Received Paper

TOTAL:

Number of Papers published in peer-reviewed journals:

(b) Papers published in non-peer-reviewed journals (N/A for none)

Received Paper

TOTAL:

Number of Papers published in non peer-reviewed journals:

(c) Presentations

Jan 2012, NREL National Wind Technology Center (NWTC) “Designing Large-Eddy Simulation of the Atmospheric Boundary Layer to Predict the Law-of-the-Wall, Part II: The Influence of the Surface Stress Model and Numerical Dissipation, and the Prediction of the von Kárman Constant.”

Dec 2011, National Oceanic and Atmospheric Administration (NOAA), Boulder, CO, “Designing Large-Eddy Simulation of the Atmospheric Boundary Layer to Predict the Law-of-the-Wall”

Nov 2011, NREL National Wind Technology Center (NWTC), Boulder, CO, “Designing Large-Eddy Simulation of the Atmospheric Boundary Layer to Predict the Law-of-the-Wall.”

Oct 2011, Mechanical Engineering Graduate Seminar Series, University of Colorado, “Improving the Accuracy of Large-Eddy Simulation of Boundary Layer Flows, with Application to the Atmospheric Boundary Layer and its Interaction with Wind Turbine Aerodynamics.”

May 2011, Risø National Laboratory for Sustainable Energy Technical University of Denmark, “Designing of Large-Eddy Simulation of the Atmospheric Boundary Layer to Predict the Law-of-the-Wall: Influence on Wind Turbine Aerodynamics.”

2011, University of Texas Austin, Institute for Computational Engineering and Sciences, "Issues in the Design of Large-Eddy Simulations that are Independent of the Model for Subfilter Scale Fluxes."

Jan 2010, Meteorology Seminar Series, Pennsylvania State University, “How to Design Large-Eddy Simulation of the Atmospheric Boundary Layer to Capture Law-of-the-Wall.”

March 2009, National Center for Atmospheric Research (NCAR), “Designing Large-Eddy Simulation of High Reynolds Number Wall-bounded Flows.”

Nov 2008, Invited Plenary Seminar at the 61st Annual Meeting of the American Physical Society Division of Fluid Dynamics, San Antonio, Texas: "Designing LES of High Reynolds Number Wall-bounded Flows."

June 2008, Fifth International Workshop on Wall-Bounded Turbulent Flows, Baltimore, MD. "Understanding a Fundamental Inaccuracy in Large-Eddy Simulation of High Reynolds Number Boundary Layers."

April 2008, Los Alamos National Laboratory, Frontiers in the Geoscience Lecture Series. "Requirements to Predict the Surface Layer with High Accuracy at high Reynolds Numbers using Large-Eddy Simulation."

Mar 2008, Penn State Engineering Science and Mechanics Seminar Series, "Requirements to Predict the Surface Layer with High Accuracy at high Reynolds Numbers using Large-Eddy Simulation."

Feb 2008, Princeton University, Dept. of Mechanical and Aerospace Engineering. "Understanding a Fundamental Inaccuracy in Large-Eddy Simulation of High Reynolds Number Boundary Layers."

Feb 2008, Cornell University Sibley School of Mechanical and Aerospace Engineering. "Requirements to Predict the Surface Layer with High Accuracy at High Reynolds Numbers using Large-Eddy Simulation."

Jan 2008, Applied Research Laboratory Seminar Series, Penn State. "Requirements to Predict the Surface Layer with High Accuracy at high Reynolds Numbers using Large-Eddy Simulation."

July 2007, Imperial College London Institute for Mathematical Sciences, “A Fundamental Explanation for the Over-prediction of Mean Shear in Large-eddy Simulation of Shear-dominated Surface Layers.”

Number of Presentations: 15.00

Non Peer-Reviewed Conference Proceeding publications (other than abstracts):

Received	Paper	
08/02/2015	4.00	James Brasseur, Tie Wei , Sanjiv Ramachandran. Predicting Law-of-the-Wall and the von Kármán Constant with LES., 16th U.S. National Congress of Theoretical and Applied Mechanics (USNCTAM), Pennsylvania State University, 27 June - 2 July, 2010.. 27-JUN-10, . : ,
TOTAL:	**1**	

Number of Non Peer-Reviewed Conference Proceeding publications (other than abstracts):

Peer-Reviewed Conference Proceeding publications (other than abstracts):

Received	Paper	
TOTAL:		

Number of Peer-Reviewed Conference Proceeding publications (other than abstracts):

(d) Manuscripts

Received	Paper	
08/02/2015	10.00	James Brasseur , Tie Wei. Designing Large-Eddy Simulation of the Turbulent Boundary Layer to Capture Law-of-the-Wall Scaling, Physics of Fluids (11 2009)
TOTAL:	**1**	

Number of Manuscripts:

Books

Received Book

TOTAL:

Received Book Chapter

TOTAL:

Patents Submitted

Patents Awarded

Awards

2010, Invited Paper by the Physics of Fluids: "Designing Large-Eddy Simulation of the Turbulent Boundary Layer to Capture Law-of-the-Wall Scaling"

2008, Invited Plenary Speaker at the 61st Annual Meeting of the American Physical Society Division of Fluid Dynamics, San Antonio, Texas.

Graduate Students

NAME	PERCENT_SUPPORTED
FTE Equivalent:	
Total Number:	

Names of Post Doctorates

NAME	PERCENT_SUPPORTED
Tie Wei	1.00
FTE Equivalent:	**1.00**
Total Number:	**1**

Names of Faculty Supported

NAME	PERCENT_SUPPORTED	National Academy Member
James Brasseur	0.10	
John Wyngaard	0.10	
FTE Equivalent:	**0.20**	
Total Number:	**2**	

Names of Under Graduate students supported

NAME	PERCENT_SUPPORTED
FTE Equivalent:	
Total Number:	

Student Metrics

This section only applies to graduating undergraduates supported by this agreement in this reporting period

The number of undergraduates funded by this agreement who graduated during this period: 0.00

The number of undergraduates funded by this agreement who graduated during this period with a degree in science, mathematics, engineering, or technology fields:..... 0.00

The number of undergraduates funded by your agreement who graduated during this period and will continue to pursue a graduate or Ph.D. degree in science, mathematics, engineering, or technology fields:..... 0.00

Number of graduating undergraduates who achieved a 3.5 GPA to 4.0 (4.0 max scale):..... 0.00

Number of graduating undergraduates funded by a DoD funded Center of Excellence grant for Education, Research and Engineering:..... 0.00

The number of undergraduates funded by your agreement who graduated during this period and intend to work for the Department of Defense 0.00

The number of undergraduates funded by your agreement who graduated during this period and will receive scholarships or fellowships for further studies in science, mathematics, engineering or technology fields:..... 0.00

Names of Personnel receiving masters degrees

NAME
Total Number:

Names of personnel receiving PHDs

NAME
Total Number:

Names of other research staff

NAME	PERCENT_SUPPORTED

FTE Equivalent:
Total Number:

Sub Contractors (DD882)

Inventions (DD882)

Scientific Progress

FOREWORD

It has been known for 20 years that LES predicts incorrectly mean velocity gradients near the ground. This serious error causes inaccuracy in other important predictions including, in the presence of convection, the entire structure of the ABL, heat, humidity and contaminant transport, and acoustic propagation. Many studies have tried to eliminate the overshoot through the SFS model, but none have been entirely successful because the mechanisms are not understood. We have finally succeeded in explaining the mechanisms underlying the overshoot and we have defined the requirements for high-accuracy LES of the ABL surface layer. These requirements include a mix of physical, numerical and modeling issues. Underlying the explanation is a crucial distinction between “numerical friction” and real friction and their similar roles. We show that numerical friction includes a mix of modeling, grid, and numerical elements that underlie the overshoot as well as poor predictions of law-of-the-wall. The interaction among the elements underlying numerical friction underlies the overshoot and high-accuracy LES of the surface layer. Underlying these primary issues are related issues that must be addressed in high-accuracy LES, including numerical instability, lower boundary condition, and details of the SFS closure prediction and grid.

STATEMENT OF THE PROBLEM STUDIED

In 1992 Mason and Thomson made the critical observation that their large-eddy simulations (LES) of the atmospheric boundary layer (ABL) did not predict correctly the mean velocity profile near the ground. They observed that gradients of mean velocity are much higher than predicted by law-of-the-wall scaling and shown by data in the part of the computational domain adjacent to the ground. They assumed that the over-prediction was a consequence of the failure of the Smagorinsky model, and showed that the over-prediction could be altered (but not removed) by adding a random solenoidal acceleration to the Navier-Stokes equation, in effect randomizing the subfilter-scale (SFS) stress divergence. In the intervening years it has been discovered that this over-prediction is a fundamental flaw in LES of the ABL when the surface layer is shear-dominated, and is particularly associated with eddy viscosity representations of SFS stress. A number of researchers have found that it is possible to reduce the degree of error either by adjusting details of the eddy viscosity representation or by adjusting the eddy viscosity closure itself. However, none have succeeded in fully eliminating the error, primarily because the mechanisms underlying the flaw are not understood.

The issue is much more serious in predicting geophysical boundary layers than simply an inaccurate prediction of mean velocity near the ground. Over-prediction of mean shear affects the prediction of turbulent kinetic energy production and directly alters turbulence structure and turbulence-driven fluxes in the part of the planetary boundary layer in which humans reside. Consequently, the application of LES to problems that require accurate prediction of meteorological events near the ground is questionable. Examples include ground-to-ground acoustic propagation, dispersion of contaminants originating at the ground, and wind speed and direction. As importantly, it has been shown that because atmospheric thermals originate at the ground in the part of the boundary layer where mean shear is over-predicted, the LES predictions of thermal structure are also incorrect under moderately convective conditions, not only near the surface but throughout the ABL, and that these errors are a direct consequence of the over-prediction of mean shear at the surface. Consequently, LES predictions of transport from the lower to upper ABL—humidity, heat, contaminants and other scalars—are fundamentally inaccurate, and could adversely affect other predictions such as cloud formation and long-range scalar dispersion.

Given the importance of near-surface predictions in geophysical flows, our program of research focused on resolving the now 23-year-old problem of inaccurate LES prediction of mean gradients in the surface layer.

SUMMARY OF THE MOST IMPORTANT RESULTS

After a long period of methodical detective work and a combination of mathematical and physical analysis combined with an extensive large-eddy simulation (LES) campaign of atmospheric boundary layer (ABL) simulations, we succeeded in solving the puzzle of why it is that large-eddy simulation of the atmospheric boundary layer over-predicts mean shear adjacent to the ground, and we have learned what elements are needed to address the problem and improve accuracy of surface layer predictions. As might be expected, the solution is multi-faceted, and we developed a series of requirements for high-accuracy LES of the ABL that involve a mix of numerical, gridding, and modeling issues. From our analysis we order the solution process into a hierarchy of inter-related issues that must be addressed for high-accuracy LES of the surface layer.

A highly comprehensive and though explanation of the background to the fundamental problem in LES, the mathematical theory we developed, the "R-ReLES" parameter space we created, and the analysis of over 100 ABL LES simulations to place results within this parameter space and validate both the theory and the fundamental explanation for the error, is given in an invited paper by the Physics of Fluids entitled "Designing Large-Eddy Simulation of the Turbulent Boundary Layer to Capture Law-of-the-Wall Scaling" by Brasseur & Wei. The paper appeared in 2010 and has attracted a great deal of attention within the large community that applies LES to the simulation of high Reynolds number wall bounded flows. This work has also lead to a large number of invited presentations at universities, national labs and meetings.

Deviations from the law-of-the-wall in mean velocity and velocity gradient in the inertial surface layer arise from a competition between the characteristic velocity and length scales and other velocity or length scales that enter either from the true fluid physics or during the conversion to the discretized dynamical system that is ultimately advanced on the computer. Turbulence motions in the surface layer at the characteristic length scale z, for example, may compete with motions at the boundary layer scale (Khanna & Brasseur 1997) or with the influences of surface friction or roughness that are characterized by the viscous and roughness length scales. If sufficiently strong, these confounding scales will alter the scaling of the mean velocity gradient in the inertial surface layer. Law-of-the-wall assumes that this is not the case and experiments in the laboratory and atmosphere have generally supported this assumption when there are no confounding scales and the ratio of the outer to viscous length and roughness scales are sufficiently large. However, when the influence of confounding characteristic scales is sufficiently strong to compete with the characteristic velocity and length scales in the inertial surface layer, deviations from LOTW result.

What we have shown is that, in the conversion from the exact continuous dynamical system to the LES discretized dynamical system that is actually advanced on the computer, additional characteristic scales are introduced into the simulated dynamics that can interfere with LOTW scaling in the surface layer when sufficiently strong. Several elements in the simulation might introduce spurious characteristic scales: (i) models of existing terms and new terms that are introduced into the governing equation, (ii) models for unknown boundary conditions, (iii) the type and order of the discretization of derivatives together with grid geometry, and (vi) algorithmic additions, for example, to maintain numerical stability. The current study has focused primarily on the influences of a spurious viscous length scale that is introduced within the computational domain by the model for the SFS stress tensor. This spurious scale is a reflection of the manner in which the net transfer of turbulence energy from resolved to subfilter scales is modeled. Whereas the interscale interactions that underlie the transfer of energy are purely inertial in reality, all practical closures for the SFS stress tensor model the net transfer of energy from the resolved scales by a dissipative mechanism that removes energy at the smallest resolved scales.

However, the SFS stress is often not the only term that is modeled in the conversion from the continuous to the discrete dynamical system. At the very high Reynolds numbers of practical interest, and at which law-of-the-wall is valid, the surface viscous layer, if it exists, cannot be resolved in a large-eddy simulation. The vertical derivatives in resolved and SFS stress therefore require that a model be supplied for the total stress at the surface. Hybrid schemes couple a RANS SFS stress model on a very high aspect ratio RANS grid in an extremely thin surface viscous layer with large-eddy simulation and SFS closure on an LES grid beginning in the lower inertial surface layer, also very near the surface. Thus, the LES part of the simulation obtains the lower boundary condition on stress from the RANS part of the simulation, which is far from exact. Nonhybrid schemes must supply a model for the total horizontal shear stress, generally written as a function of resolved velocity within the computational domain. So, in addition to any spurious scales introduced within the computational domain by the SFS stress model, there exists the possibility that the model for surface shear stress might introduce spurious scales at the boundary of the LES computational domain.

We have found experimentally that standard surface stress models do introduce spurious effects that force deviations from LOTW at the first couple grid levels adjacent to the surface. Fig. 10 shows that this additional confounding contribution from the lower stress boundary condition is obscured when the frictional contribution from the interior SFS stress is sufficiently overwhelming to produce the overshoot. When the LES is moved into the HAZ so that the viscous effects causing the overshoot are suppressed, the confounding influences of the surface stress model become apparent and spread vertically as the relative contribution from the interior SFS stress model diminishes with increasing R. We have also shown that adjustments to surface shear stress are possible which significantly reduce the spurious influence of standard surface stress models

BIBLIOGRAPHY

Brasseur, J.G., Wei, T. 2010 Designing Large-Eddy Simulation of the Turbulent Boundary Layer to Capture Law-of-the-Wall Scaling, Physics of Fluids 22: 021303-1 - 021303-21: Invited Paper.

Khanna, S., Brasseur, J.G. 1998 Three dimensional buoyancy- and shear-induced structure of the atmospheric boundary layer. J. Atmos. Sciences 55: 710-743.

Khanna, S., Brasseur, J.G. 1997 Analysis of Monin-Obukhov similarity from large-eddy simulation. J. Fluid Mech. 345: 251-286.

Technology Transfer

Final Report
July 2015

HIGH-ACCURACY NEAR-SURFACE LARGE-EDDY SIMULATION WITH PLANAR TOPOGRAPHY

ARO Grant W911NF-04-1-0205

PI: James G. Brasseur

FOREWORD

It has been known for 20 years that large-eddy simulation (LES) predicts incorrectly mean velocity gradients near the ground. This serious error causes inaccuracy in other important predictions including, in the presence of convection, the entire structure of the atmospheric boundary layer (ABL), heat, humidity and contaminant transport, and acoustic propagation. Many studies have tried to eliminate the overshoot through the SFS model, but none have been entirely successful because the mechanisms are not understood. We have finally succeeded in explaining the mechanisms underlying the overshoot and we have defined the requirements for high-accuracy LES of the ABL surface layer. These requirements include a mix of physical, numerical and modeling issues. Underlying the explanation is a crucial distinction between "numerical friction" and real friction and their similar roles. We show that numerical friction includes a mix of modeling, grid, and numerical elements that underlie the overshoot as well as poor predictions of law-of-the-wall. The interaction among the elements underlying numerical friction underlies the overshoot and high-accuracy LES of the surface layer. Underlying these primary issues are related issues that must be addressed in high-accuracy LES, including numerical instability, lower boundary condition, and details of the SFS closure prediction and grid.

STATEMENT OF THE PROBLEM STUDIED

In 1992 Mason and Thomson made the critical observation that their large-eddy simulations of the atmospheric boundary layer (ABL) did not predict correctly the mean velocity profile near the ground. The pointed out that the mean velocity gradient scaled according to inertial Law-of-the-Wall (LOTW) scaling,

$$\phi(z) \equiv \frac{z}{u_*}\frac{\partial U}{\partial z}, \tag{1}$$

produces a well-defined peak within the surface layer; the LES does not predict the LOTW. This "overshoot" has since been pointed out and studied by many researchers.

Mason and Thomson assumed that the over prediction of gradients of mean velocity relative to law-of-the-wall scaling and shown by data in the part of the computational domain adjacent to the ground is a consequence of the failure of the Smagorinsky model, and showed that the over-prediction could be altered (but not removed) by adding a random solenoidal acceleration to the Navier-Stokes equation, in effect randomizing the subfilter-scale (SFS) stress divergence. In the intervening years it has been discovered that this over-prediction is a fundamental flaw in LES of the ABL when the surface layer is shear-dominated, and is particularly associated with eddy viscosity representations of SFS stress. A number of researchers have found that it is possible to reduce the degree of error either by adjusting details of the eddy viscosity representation or by adjusting the eddy viscosity closure itself. However, none have succeeded in fully eliminating the error, primarily because the mechanisms underlying the flaw are not understood.

The issue is much more serious in predicting geophysical boundary layers than simply an inaccurate prediction of mean velocity near the ground. Over-prediction of mean shear affects the prediction of turbulent kinetic energy production and directly alters turbulence structure and turbulence-driven fluxes in the part of the planetary boundary layer in which humans reside. Consequently, the application of LES to problems that require accurate prediction of meteorological events near the ground is questionable. Examples include ground-to-ground acoustic propagation, dispersion of contaminants originating at the

ground, and wind speed and direction. As importantly, it has been shown that because atmospheric thermals originate at the ground in the part of the boundary layer where mean shear is over-predicted, the LES predictions of thermal structure are also incorrect under moderately convective conditions, not only near the surface but throughout the ABL, and that these errors are a direct consequence of the over-prediction of mean shear at the surface. Consequently, LES predictions of transport from the lower to upper ABL—humidity, heat, contaminants and other scalars—are fundamentally inaccurate, and could adversely affect other predictions such as cloud formation and long-range scalar dispersion.

Given the importance of near-surface predictions in geophysical flows, our program of research focused on resolving the now 23-year-old problem of inaccurate LES prediction of mean gradients in the surface layer.

SUMMARY OF THE MOST IMPORTANT RESULTS

After a long period of methodical detective work and a combination of mathematical and physical analysis combined with an extensive large-eddy simulation (LES) campaign of atmospheric boundary layer (ABL) simulations, we succeeded in solving the puzzle of why it is that large-eddy simulation of the atmospheric boundary layer over-predicts mean shear adjacent to the ground, and we have learned what elements are needed to address the problem and improve accuracy of surface layer predictions. As might be expected, the solution is multi-faceted, and we developed a series of requirements for high-accuracy LES of the ABL that involve a mix of numerical, gridding, and modeling issues. From our analysis we order the solution process into a hierarchy of inter-related issues that must be addressed for high-accuracy LES of the surface layer.

A highly comprehensive and though explanation of the background to the fundamental problem in LES, the mathematical theory we developed, the "R-ReLES" parameter space we created, and the analysis of over 100 ABL LES simulations to place results within this parameter space and validate both the theory and the fundamental explanation for the error, is given in an invited paper by the Physics of Fluids entitled "Designing Large-Eddy Simulation of the Turbulent Boundary Layer to Capture Law-of-the-Wall Scaling" by Brasseur & Wei. The paper appeared in 2010 and has attracted a great deal of attention within the large community that applies LES to the simulation of high Reynolds number wall bounded flows. This work has also lead to a large number of invited presentations at universities, national labs and meetings.

Deviations from the law-of-the-wall in mean velocity and velocity gradient in the inertial surface layer arise from a competition between the characteristic velocity and length scales and other velocity or length scales that enter either from the true fluid physics or during the conversion to the discretized dynamical system that is ultimately advanced on the computer. Turbulence motions in the surface layer at the characteristic length scale z, for example, may compete with motions at the boundary layer scale (Khanna & Brasseur 1997) or with the influences of surface friction or roughness that are characterized by the viscous and roughness length scales. If sufficiently strong, these confounding scales will alter the scaling of the mean velocity gradient in the inertial surface layer. Law-of-the-wall assumes that this is not the case and experiments in the laboratory and atmosphere have generally supported this assumption when there are no confounding scales and the ratio of the outer to viscous length and roughness scales are sufficiently large. However, when the influence of confounding characteristic scales is sufficiently strong to compete with the characteristic velocity and length scales in the inertial surface layer, deviations from LOTW result.

What we have shown is that, in the conversion from the exact continuous dynamical system to the LES discretized dynamical system that is actually advanced on the computer, additional characteristic scales are introduced into the simulated dynamics that can interfere with LOTW scaling in the surface layer when sufficiently strong. Several elements in the simulation might introduce spurious characteristic scales: (i) models of existing terms and new terms that are introduced into the governing equation, (ii) models for unknown boundary conditions, (iii) the type and order of the discretization of derivatives together with grid geometry, and (vi) algorithmic additions, for example, to maintain numerical stability. The current study has focused primarily on the influences of a spurious viscous length scale that is introduced within the computational domain by the model for the SFS stress tensor. This spurious scale is a reflection of the manner in which the net transfer of turbulence energy from resolved to subfilter scales is modeled. Whereas the interscale interactions that underlie the transfer of energy are purely inertial in

reality, all practical closures for the SFS stress tensor model the net transfer of energy from the resolved scales by a dissipative mechanism that removes energy at the smallest resolved scales.

However, the SFS stress is often not the only term that is modeled in the conversion from the continuous to the discrete dynamical system. At the very high Reynolds numbers of practical interest, and at which law-of-the-wall is valid, the surface viscous layer, if it exists, cannot be resolved in a large-eddy simulation. The vertical derivatives in resolved and SFS stress therefore require that a model be supplied for the total stress at the surface. Hybrid schemes couple a RANS SFS stress model on a very high aspect ratio RANS grid in an extremely thin surface viscous layer with large-eddy simulation and SFS closure on an LES grid beginning in the lower inertial surface layer, also very near the surface. Thus, the LES part of the simulation obtains the lower boundary condition on stress from the RANS part of the simulation, which is far from exact. Nonhybrid schemes must supply a model for the total horizontal shear stress, generally written as a function of resolved velocity within the computational domain. So, in addition to any spurious scales introduced within the computational domain by the SFS stress model, there exists the possibility that the model for surface shear stress might introduce spurious scales at the boundary of the LES computational domain.

We have found experimentally that standard surface stress models do introduce spurious effects that force deviations from LOTW at the first couple grid levels adjacent to the surface. Fig. 10 shows that this additional confounding contribution from the lower stress boundary condition is obscured when the frictional contribution from the interior SFS stress is sufficiently overwhelming to produce the overshoot. When the LES is moved into the HAZ so that the viscous effects causing the overshoot are suppressed, the confounding influences of the surface stress model become apparent and spread vertically as the relative contribution from the interior SFS stress model diminishes with increasing R. We have also shown that adjustments to surface shear stress are possible which significantly reduce the spurious influence of standard surface stress models

DETAILS OF THE ANALYSES DEVELOPED AND SOLUTIONS ACHIEVED

I. Background on "the Overshoot problem"

Before developing our analysis into essential mechanisms underlying the prediction of LOTW scaling of mean velocity gradient in the surface layer with large-eddy simulation, we set the stage with discussion into the overshoot and its history. Previous studies, many of which have produced significant reductions in the degree of overshoot, have provided important clues that lead to the theory developed here, and present results that a theory should explain.

A. Consequences of an overshoot in mean shear rate

Figure 1 shows essential aspects of the overshoot from several previous large-eddy simulations of the neutral boundary layer that have focused on this issue since Mason & Thomson[1]. Because the overshoot is associated with the shear-dominated region of the boundary layer, it is particularly apparent in the fully shear-driven neutral boundary layer (Fig. 1). Piomelli and Balaras[16] point out that in DES of the shear-driven boundary layer, "unphysical, nearly one-dimensional, wall streaks were present in the RANS region … and shorter-scale outer-layer eddies were progressively formed as one moved away from the wall." Similar observations have been made in the neutral atmospheric boundary layer[17].

In the moderately convective atmospheric boundary layer an overshoot is produced in the shear-dominated surface layer while the mixed layer is buoyancy dominated[18]. In the presence of convection, vertically driven thermals couple the surface and outer boundary layers. Khanna & Brasseur[17] showed that the elongated structure of streamwise turbulence fluctuations generated near the surface by the interaction between strong mean shear and turbulence (streaks) are the source of thermals that penetrate the outer boundary layer. These coherent elongated vertical motions interact with the horizontal mean wind to form highly coherent secondary rolls that extend to the top of the boundary layer and can extend 20-40 boundary layer thicknesses in the mean wind direction[19]. Thus, there is a direct coupling between the near-surface shear-driven streaks and very large eddy structure of the boundary layer. (It is possible that

the mechanisms that underlie the creation of the longitudinal convective rolls may be related to the mechanisms underlying much weaker highly elongated structures that have been observed in the log layer of the neutral boundary layer[20].)

An important negative consequence of the inner-outer coupling is that the near-surface errors from the overshoot are driven vertically to infect the entire boundary layer. To demonstrate this, Khanna & Brasseur[17] applied two SFS models to the same LES; one produced a stronger overshoot than the other. The LES with the stronger overshoot produced much stronger and coherent convective thermals and boundary layer rolls with much larger horizontal integral scales that persisted to the top of the boundary layer. Furthermore, these overly coherent thermals are spuriously aligned with the mean geostrophic wind. This spuriously strong thermal structure will adversely influence vertical transport to the upper atmosphere of momentum, thermal energy, contaminants, and humidity. Error in humidity predictions will likely enter cloud cover predictions and produce error in solar radiative heating at the earth's surface. Incorrect prediction of vertical transport of CO_2 and other greenhouse gases may affect related predictions of upper atmosphere chemistry.

The negative consequences of the overshoot in mean velocity gradient arise essentially from the incorrect prediction of Reynolds stress anisotropy near the surface. Juneja & Brasseur[21] argued that the incorrect anisotropy results from a feedback interaction between the exaggerated mean gradient and Reynolds stress production as a consequence of inherent under-resolution at the first grid level that occurs in LES of high Reynolds number turbulent boundary layers when the first grid level is in the inertial layer. The errors are exacerbated by any mechanism that enhances vertical transport, including buoyancy[17] and boundary layer separation.

B. Previous studies

Given the fundamental importance of the overshoot, there have been a number of studies that have attempted either to understand the cause of the overshoot[21], or have attempted to remove it. Mason and Thomson[1], for example, suggested that the overshoot is particular to eddy viscosity closures where energy is removed at each point from the resolved scales in contrast with the known forward/backward nature of energy transfer at a point. To introduce "backscatter" into the simulation, they added to the resolved momentum equation a Langevin-like stochastic acceleration term, in addition to a SFS stress divergence using the Smagorinsky closure for SFS stress. However, Mason & Thomson[1] made another significant modification—they reduced the eddy viscosity near the surface by making the Smagorinsky length scale proportional to z at grid nodes near the surface.

In Fig. 1 we compare results from four other groups of researchers between 1994 and 2005 who explicitly addressed the problem of the overshoot in LES of the ABL. The surface layer is shaded to indicate the region over which Φ_m should be predicted as a straight vertical line and from which a grid-independent prediction for mean velocity should emanate. Fig. 1(a) shows predictions from Sullivan *et al*[11] who argued that, as the surface is approached, the SFS stress closure should transition from an eddy viscosity model appropriate to LES to a model more appropriate to the Reynolds-averaged Navier-Stokes equation (RANS). Although their mixed eddy viscosity model was purely dissipative (no backscatter), the overshoot was significantly reduced compared to a pure SFS model. Like Mason & Thomson[1], their mixed model results in a reduction in net SFS stress and eddy viscosity near the surface. Whereas the overshoot could be reduced, and perhaps even eliminated, by the adjustments to the SFS model, a dependence of $\phi(z)$ on z persisted (Fig 1(a)). The Sullivan *et al.*[11] model was further modified by Ding *et al.*[22]. Recently, Leveque *et al.*[23] modified the Smagorinsky eddy-viscosity by subtracting mean shear from the instantaneous resolved rate-of-strain tensor. Whereas they applied the model only to low Reynolds number boundary layers with partially resolved viscous layers, the effect is again to reduce the eddy viscosity near the surface. However the LES predictions failed to predict constant $\phi(z)$ over the entire surface layer.

Kosovic[24] added additional nonlinear terms in velocity gradient to the eddy viscosity closure. Whereas major improvement in the overshoot in the neutral ABL was obtained (Fig. 1(b)), grid resolution was quite low and the improvement degraded at higher grid resolution. Dynamic formulations of the Smagorinsky eddy viscosity closure have been applied by Porté-Agel *et al.*[25] and Esau[26] to improve the overshoot and capture the LOTW. We show in Fig. 1(c) results from Porté-Agel *et al.*[25] who developed a

scale-dependent formulation of the dynamic Smagorinsky model that produces a reduction in eddy viscosity near the surface and removes an apparent undershoot with the standard dynamic model (solid line). Whereas the modifications significantly reduced the overshoot, constant $\phi(z)$ was not obtained over the surface layer.

Chow *et al.*[27] combined a number of modeling elements, including a dynamic eddy viscosity model[28], a "resolvable subfilter scale stress model" component[29] combined with a deconvolution procedure[30], and a "canopy model"[31]. As shown in Fig. 1(d), whereas over-prediction of mean shear near the surface could be reduced with certain combinations of elements, it was not clear which modeling elements were responsible, and a robust grid-independent solution was not obtained. A recent calculation by Drobinski *et al.*[32], however, indicated that a suppression of the overshoot was possible using a standard one-equation model but with a more refined grid. Their result will be discussed in Sects. VI.B and VII.B in context with the current analysis.

Figure 2 shows that what we refer to here as an "overshoot" is described as a "logarithmic layer mismatch" or "super buffer layer" in the detached-eddy simulations of Nikitin *et al.*[14]. Spalart[15] and Piomelli and Balaras[16] described this as a fundamental unresolved problem in DES. Whereas the simulations of Fig. 1 contain only the inertial LOTW layer due to the presence of surface roughness and the fluctuating surface stress is modeled, the DES simulations used RANS to model a viscous surface layer with no slip at the wall (shown in Fig. 2(a)) below an inertial-dominated surface layer that is simulated with LES, as shown in Fig. 2(b). The logarithmic layer mismatch, shown by the circled part of the mean velocity profile Fig. 2(a), is shown in Fig. 2(b) to be equivalent to the overshoot phenomenon discussed above.

Figures 1 and 2 motivate the current research; we seek an understanding of the essential mechanisms underlying the overshoot that will both eliminate the overshoot and predict a vertical line in Φ_m vs. z over the entire surface layer with a grid-independent prediction over the entire boundary layer. Historically, the assumption has been that the solution to the overshoot problem is strictly a closure issue and all attempts to modify LES to predict LOTW have been through adjustments to the SFS stress tensor model. Although there have been significant advances made, the fundamental mechanisms underlying the overshoot are not understood so that a clear path to robust grid-independent LES that eliminates the overshoot and predicts LOTW scaling has been elusive. We show here that the fundamental issues underlying the overshoot and its resolution are broader than the SFS model and involve basic characteristics of the SFS stress closure integrated with the construction of the LES grid.

C. Useful clues

In the studies described above, a number of important observations have been made that provide clues to underlying issues and which require explanation:

1. The overshoot is influenced by the details of the SFS model. This has been discussed above in Sect. II.B (Fig. 1). Whereas there have been many variants to the modeling process, all have employed an eddy viscosity component. A common characteristic of the more successful adjustments to the modeling process is a reduction in eddy viscosity near the surface compared to unadulterated models.

2. The overshoot is tied to the grid. Khanna & Brasseur[18] pointed out that increasing the resolution of the grid, keeping all other elements of the simulation unchanged, does not diminish the magnitude of the overshoot, but moves the peak in Φ_m closer to the surface in proportion to the vertical grid spacing , Δ_z. Similarly, Spalart[15] pointed out that in DES "grid refinement merely moves the same amount of [logarithmic layer] mismatch closer to the wall." This dependence of the overshoot on grid resolution is clear, for example, in Fig. 1(d). Why the location of the overshoot should be proportional to Δ_z, however, is not understood. Khanna & Brasseur[18] pointed out that, because the horizontal integral scale of vertical velocity scales on z, vertical velocity is always under-resolved at the first grid level independent of grid resolution and that this under-resolution has negative consequences that must be addressed to eliminate the overshoot. Specifically, they proposed that this inherent under-resolution at the first grid level somehow ties the overshoot to the grid. The mechanisms were unclear, but were felt to be somehow associated with the lack of performance of SFS models when the integral scales are under resolved. This shall be discussed in Sec. IV.B.

3. The prediction of mean velocity gradient is grid-dependent. A requirement for any successful numerical simulation is grid independence in the solution for mean variables[33]. As illustrated in Fig. 1(d), the solution for mean velocity gradient often does not converge as the grid is refined; each grid produces a different solution not only in the overshoot region but throughout the boundary layer. Grid dependence in the flow is apparent when different solutions in the literature are compared (e.g., Andren *et al.*[10]). We shall show in Sect. VI.C that a grid-independent solution is only possible when both the overshoot is suppressed and LOTW scaling are obtained.

It is apparent from these previous studies that although the overshoot is influenced by the closure for SFS stress, the overshoot problem is only part of the broader issue of accurately predicting the LOTW, and that these are both modeling and numerical issues.

II. An Analysis of the fundamental Nature of the Overshoot: the First observation

In this section we focus specifically on the overshoot. A primary mechanism underlying the overshoot and its resolution can be understood by comparing true inertial-vs.-viscous scaling underlying the stationary fully developed smooth-wall channel flow in the high Reynolds number limit with scaling of large-eddy simulation of the same high Reynolds number channel flow with unresolved viscous or roughness layer. We shall find that we can relate the true physics of the channel flow to the spurious physics of the simulated channel flow that is model and algorithmically dependent and cannot be entirely eliminated.

A. Scaling high Reynolds number smooth wall turbulent channel flow

Consider a fully developed stationary smooth wall incompressible channel flow at Reynolds numbers sufficiently high to support the classical LOTW in the surface layer. The local and global mean axial momentum balances are, respectively,

$$\frac{\partial P}{\partial x}=\frac{\partial T_t(z)}{\partial z}+\frac{\partial T_\nu(z)}{\partial z}=\frac{\partial T_{tot}(z)}{\partial z} \text{ and } \frac{\partial P}{\partial x}=-\frac{T_0}{\delta}, \tag{2}$$

where $T_0 \equiv T_{tot}(0) \equiv \rho u_*^2$ and δ is the half channel width, or boundary layer depth (the height where $T_{tot}=0$). The second expression in (2) results from a global force balance. The coordinates (x,y,z) are in the mean-flow, spanwise, and wall-normal directions, respectively. $P(x)$ is the mean pressure, and $T_{tot}=T_t+T_\nu$ is the total mean stress, where T_t and T_ν are Reynolds stress and mean viscous stress, respectively:

$$T_t(z)=-\rho\langle u'w'\rangle, \quad T_\nu(z)=\mu\frac{\partial U}{\partial z}. \tag{3}$$

Capital letters and primed quantities indicate mean flow and fluctuating variables, respectively, (u,v,w) are the velocity components in the (x,y,z) directions, (ρ,μ) are density and viscosity, and the angle brackets denote ensemble averaging.

Integrating Eq. (2) in z and replacing $T_\nu(z)$ with $\frac{\mu u_*}{\kappa z}\Phi_m(z)$, the exact equation for the normalized mean gradient is

$$\Phi_m(z)=\kappa z^+\left(1-T_t^+(z)-\frac{z}{\delta}\right), \tag{4}$$

where $T_t^+=T_t/T_0$ is the ratio of the Reynolds stress $T_t(z)$ to the wall stress T_0, and $z^+=z/\ell_\nu$ is the surface-normal coordinate nondimensionalized by the *viscous* surface layer scale $\ell_\nu=\nu/u_*$, where $\nu=\mu/\rho$. Equation (4) states that the total stress $T_{tot}(z)$, split between the viscous and inertial contributions on LHS and RHS of (4), decreases linearly from T_0 at the surface to zero at the channel center-plane. Near

the surface ($z/\delta << 1$) in the friction-dominated layer ($z^+ \lesssim 5$), the turbulent stress is negligible ($T_t^+ << 1$) and Eq. (4) is well approximated by

$$\Phi_m(z) \approx \kappa z^+ \qquad (z^+ \lesssim 5). \tag{5}$$

This result suggests that $\Phi_m(z)$ exceeds 1 when $z^+ > 1/\kappa \approx 2.5$ (for $\kappa \approx 0.4$), which is well within the friction-dominated portion of the surface layer.

Equation (5) indicates that an overshoot in $\Phi_m(z)$ exists in the smooth-surface high Reynolds number channel flow in a region bounded from below by $z^+ \approx 2.5$ and from above by the lower margin of the inertial LOTW layer and upper margin of the buffer layer. In Fig. 3 we show that this is indeed the case. We replot, in this figure, data from direct numerical simulations (DNS) of the smooth-wall channel at different Reynolds numbers that has been graciously made available to the scientific community by Iwamoto *et al.*[34,35] at Re_τ = 300, 395, and 642, and at Re_τ = 2003 by Hoyas & Jimenez[36], where $\mathrm{Re}_\tau = u_*\delta/\nu$. Figure 3(a) shows that $\Phi_m(z^+)$ exceeds 1 when z^+ exceeds ≈2.5 and peaks at $z^+ \approx 10$ with a maximum value of about 2.3 independent of Reynolds number. Φ_m approaches 1 at $z^+ \approx$ 40-50. Comparing Fig. 3(c) with Fig. 3(d), it is significant that the peak in $\Phi_m(z)$ occurs nearly coincident with the crossover between turbulent stress $T_t(z)$ and viscous stress $T_\nu(z)$. Both the location of overshoot and the location of the crossover occur at $\approx 10\,\ell_\nu$. Since the position of this overshoot scales on the viscous scale and corresponds to the transition between the dominance of turbulent stress above and viscous stress below, this overshoot reflects the application of an *inertial* length scale z in the portion of the surface layer where the appropriate length scale is the *viscous* surface scale ℓ_ν. Fig. 3(c) and Fig. 3(d) show that the overshoot and the crossover in $T_\nu(z)$ and $T_t(z)$, move physically closer to the surface with increasing Reynolds number without a reduction in maximum Φ_m.

B. LES of high Reynolds number turbulent channel flow

We compare the previous analysis with large-eddy simulation of the same high Reynolds number channel flow analyzed in Sect. III.A, but in which either a viscous layer exists that is fully unresolved ($\ell_\nu << \Delta_z$) or the surface is rough with fully unresolved roughness scale ($z_0 \ll \Delta_z$). The momentum equation for the resolved velocity u_i^r is

$$\frac{\partial u_i^r}{\partial t} + \frac{\partial (u_i^r u_j^r)}{\partial x_j} = -\frac{1}{\rho}\frac{\partial p^r}{\partial x_i} - \frac{\partial \tau_{ij}^{SFS}}{\partial x_j}\ , \tag{6}$$

where the viscous force has been scaled out of the momentum balance on account of the high local Reynolds numbers on all grid nodes within the computational domain (surface viscous layers are unresolved or nonexistence). The subfilter-scale (SFS) stress tensor τ_{ij}^{SFS} is modeled. We apply a superscript *r* to indicate a variable that is carried forward in the simulation as a resolved variable—that is, after the process of explicit and implicit filtering in the algorithmic advancement of the modeled discretized version of Eq. (6). Explicit filtering is generally carried out algorithmically as a dealiasing step[1], typically in pseudo-spectral LES. Implicit filtering arises from the dissipative nature of the model for τ_{ij}^{SFS}, from numerical dissipation within the discretized version of Eq. (6), and from any dissipative elements introduced algorithmically as the discretized dynamical system is advanced in time.

The ensemble mean of Eq. (6) for stationary fully developed high Reynolds number channel flow is:

---

[1] Algorithmically, $(u^r u^r)$ in equation (6) should be written as $(u^r u^r)^{\hat{r}}$ to indicate the common application of a second explicit filter $\hat{r}$ on the nonlinear term.

$$\frac{\partial P}{\partial x} = \frac{\partial T_R(z)}{\partial z} + \frac{\partial T_S(z)}{\partial z} = \frac{\partial T_{tot}(z)}{\partial z}, \text{ with } \frac{\partial P}{\partial x} = -\frac{\rho u_*^2}{\delta}, \tag{7}$$

where $T_0 \equiv T_{tot}(0) \equiv \rho u_*^2$. The second equation is the global force balance. Total stress $T_{tot} = T_R + T_S$ is now the summation of a turbulent stress T_R formed from the fluctuating resolved velocity components and the shear component of the mean SFS stress tensor, T_S:

$$T_R(z) = -\rho\left\langle u^{r\prime} w^{r\prime} \right\rangle,\ T_S(z) = -\rho\left\langle \tau_{13}^{SFS} \right\rangle. \tag{8}$$

Whereas the divergence of the SFS "stress" is physically an inertial contribution to the force balance, in application all SFS models are structured so as to contain a frictional contribution to the equation of motion. This is explicitly true of eddy viscosity models and mixed models which include an eddy viscosity term.

In what follows, we do not restrict our theoretical treatment to any particular SFS stress model. We do, however, use eddy viscosity closures for guidance and to carry out numerical experiments.

We seek a mechanism to extract the frictional component of the complete modeled tensor τ_{ij}^{SFS}; that is, we seek an estimate of a scalar viscosity that extracts the part of τ_{ij}^{SFS} that is parallel to the resolved strain-rate tensor, s_{ij}^r, in the mean. For the purposes of determining the underlying causes of the overshoot in the highly shear-dominated part of the boundary layer, we define a "LES viscosity," $\nu_{les}(z)$, as the proportionality between $-\rho\left\langle \tau_{13}^{SFS} \right\rangle$ and $2\left\langle s_{13}^r \right\rangle = \partial U / \partial z$:

$$\nu_{les}(z) \equiv \frac{T_S(z)}{2\rho\left\langle s_{13}^r \right\rangle}, \qquad \text{(closure independent)} \tag{9}$$

where s_{ij}^r is the resolved strain-rate tensor. Furthermore, since we are focused on the first few grid points adjacent to the surface, we parameterize LES viscosity with its value at the first grid level, $\nu_{LES}(z_1)$, and we define the normalized LES viscosity as follows:

$$\nu_{LES} \equiv \nu_{les}(z_1), \quad \nu_{les}^+(z) \equiv \frac{\nu_{les}(z)}{\nu_{LES}}. \tag{10}$$

We emphasize that the definitions in (9) and (10) do not assume an eddy viscosity model and can be made for *any* closure of the SFS stress tensor. However, this estimate of frictional content does is only valid with strong mean shear at the first grid level, and is therefore appropriate to the neutral boundary layer, and the stable and moderately convective atmospheric boundary layers with shear-dominated turbulence at z_1.

Replacing T_S in Eq. (7) with $\rho\nu_{LES}\nu_{les}^+(z)\dfrac{\partial U}{\partial z}$, integrating in z, and using inertial LOTW scaling (Eq. 1), produces the following expression for $\Phi_m(z)$:

$$\Phi_m(z) = \frac{\kappa z_{LES}^+}{\nu_{les}^+(z)}\left(1 - T_R^+(z) - \frac{z}{\delta}\right), \tag{11}$$

where

$$z_{LES}^+ \equiv \frac{z}{\ell_{\nu_{LES}}},\ \ell_{\nu_{LES}} \equiv \frac{\nu_{LES}}{u_*},\ \text{ and }\ T_R^+ \equiv \frac{T_R}{T_0}. \tag{12}$$

As in the exact channel flow equations, $T_0 = T_{tot}(0) \equiv \rho u_*^2$, so that $T_R^+(z)$ is the ratio of the resolved part of the Reynolds shear stress to the total wall shear stress. Unlike the viscous layer where we could argue that the Reynolds stress is a small percentage of wall stress and approximate Eq. (4) by Eq. (2), we cannot

a-priori argue that $T_R << T_0$. However, at the first few grid points, $z/\delta << 1$ and $\nu^+_{les}(z) \sim O(1)$, so that (11) can be approximated by

$$\Phi_m(z) \approx \kappa z^+_{LES}\left(1 - T^+_R\right) \quad \text{(first few grid points)}. \tag{13}$$

The magnitude of T^+_R depends on the relative content of resolved to SFS stress in total stress $T_{tot} = T_R + T_S$. When the separation between resolved and subfilter-scales takes place in the inertial range of turbulence scales, implying that all integral scales are well resolved, then $T_S << T_R$, and T^+_R cannot be neglected in Eq. (13). However, as discussed in Sect. II.C, some integral scales are inherently under-resolved at the first few grid levels in high Reynolds number LES of wall-bounded flows. Thus, it may be the case that $T^+_R << 1$ close to the surface so that Eq. (13) is approximated by $\Phi_m(z) \approx \kappa z^+_{LES}$. If this were the case, then we would reach the same conclusion as when Eq. (4) was reduced to Eq. (5) in the viscous sublayer of the smooth-wall channel flow: an overshoot would occur when $z^+_{LES} \gtrsim 1/\kappa \approx 2.5$, that is when $z \gtrsim 2.5\ell_{\nu_{LES}}$.

Figure 4 shows that, indeed, $T_S \gg T_R$ near the surface in a typical LES of the neutral atmospheric boundary layer[2] using the Smagorinsky model, so that $\Phi_m(z) \approx \kappa z^+_{LES}$ and an overshoot is produced at $z^+_{LES} \gtrsim 2.5$. In fact, Fig. 4(a,b) is very similar to the curves in Fig. 3(a,b) of the real overshoot in the smooth wall channel flow. The spurious overshoot initiates between the first and second grid levels and peaks nearly coincident with the crossover between T_R and T_S, very similar to Fig. 3 where the real overshoot is found to be coincident with the crossover between T_t and T_ν.

The overshoot in LES appears to arise from physics similar to the true overshoot in smooth wall channel flow. However, in LES the frictional layer that causes the overshoot is a *numerical LES frictional layer* near the surface that arises from the frictional nature of the modeled SFS stress (and any numerical and algorithmic additions to dissipation). This conclusion analyzed further in the following sections.

C. The first criterion

The observation from Fig. 4 that the overshoot is associated with a reduction in the resolved Reynolds stress to below the mean SFS stress suggests that the spurious frictional content of the model for SFS stress has introduced a spurious length scale $\ell_{\nu_{LES}}$ that interferes with the inertial scale z that should dominate the surface layer. The spurious interference of $\ell_{\nu_{LES}}$ with inertial scaling and the consequent spurious overshoot are essentially the same physics that underlie the production of the real overshoot in the friction-dominated part of the LOTW layer of the smooth-wall channel flow. However, unlike the true viscous layer, which is a necessary consequence of frictional force with no-slip, the spurious LES frictional layer must be controlled to eliminate the frictionally induced spuriously large mean gradients near the surface. If it were possible to maintain the dominance of T_R over T_S to the surface, then the spurious frictional contribution from the SFS stress model would remain suppressed. This observation suggests a criterion for elimination of the overshoot, that

$$\Re \equiv \frac{T_{R_1}}{T_{S_1}} > \Re^* \sim O(1), \qquad \text{(closure independent)} \tag{14}$$

where the subscripts 1 mean "at the first grid level." The critical value $\Re^*$, to be determined experimentally, is an order 1 quantity but may depend on the model for SFS stress, the lower boundary condition, the stability of the ABL, the numerical algorithm, etc.

[2] We describe the details of our large-eddy simulations of the atmospheric boundary layer in Appendix B.

D. Understanding the ratio $\Re$ and the first criterion

On what does $\Re$ depend and how can it be controlled in a large-eddy simulation? To gain insight into the nature of $\Re$ and find an answer to this question, we develop expressions for $\Re$ based on eddy viscosity representations for the deviatoric part of the SFS stress, $[\tau_{ij}^{SFS}]_{dev} \equiv \tau_{ij}^{SFS} - [\tau_{kk}^{SFS}/3]\delta_{ij}$:

$$[\tau_{ij}^{SFS}]_{dev} = -2\nu_t s_{ij}^r \ , \ \ \nu_t = \ell_t u_t \, , \tag{15}$$

where ℓ_t and u_t^2 characterize length and energy at the smallest resolved scales. ℓ_t is often taken as a fixed length scale $\ell_t = C_t\Delta$, where $\Delta = (\Delta_x\Delta_y\Delta_z)^{1/3}$ is the grid size ($\Delta_x, \Delta_y, \Delta_z$ are the grid spacings in *x,y,z*) and C_t is a model constant. Some models embed *z*-dependence into ℓ_t in the form $\ell_t(z) = C_t\tilde{\ell}_t(z)$, where $\tilde{\ell}_t(z)$ is specified to decrease towards the surface and approaches Δ away from the surface[1]. Dynamic models take $\ell_t = C_t\Delta$, but determine C_t dynamically with the result that $C_t = C_t(z)$ reduces near the surface[25]. Thus, in each case the modeled length scale $\ell_t(z)$ decreases towards the surface. In the current work we develop scaling from eddy viscosity closures with constant $\ell_t = C_t\Delta$, but shall discuss our results in context with z-dependent ℓ_t in the Discussion, Sect.VII.B.

The space-time variability in $\nu_t(\mathbf{x},t)$ is modeled through a fluctuating velocity scale $u_t(\mathbf{x},t)$, given for the Smagorinsky closure by $u_{t,smag}(\mathbf{x},t) = \Delta(2s_{ij}^r s_{ij}^r)^{1/2}$. In the basic one-equation model $u_{t,1-eq}(\mathbf{x},t) = \sqrt{e(\mathbf{x},t)}$, where $e(\mathbf{x},t)$ represents the SFS kinetic energy, modeled through a prognostic equation[37,32]. In both models $\ell_t = C_t\Delta$. Here we develop expressions using the Smagorinsky closure with C_t replaced by C_s^2, as is traditional. However we shall present results for both the Smagorinsky and one-equation eddy viscosity models.

Independent of the model, $[\tau_{13}^{SFS}]_{dev} = \tau_{13}^{SFS}$ and

$$T_{S_1} = -\rho\left\langle \tau_{13}^{SFS} \right\rangle_1 \equiv 2\rho\nu_{LES}\left\langle s_{13}^r \right\rangle_1 = 2\rho\xi_1\left\langle \nu_t \right\rangle_1\left\langle s_{13}^r \right\rangle_1 , \tag{16}$$

where

$$\nu_{LES} = \xi_1\left\langle \nu_t \right\rangle_1 \text{ with } \xi_1 = \left(1 + \frac{\left\langle \nu_t' s_{13}^{r\,\prime} \right\rangle_1}{\left\langle \nu_t \right\rangle_1\left\langle s_{13}^r \right\rangle_1} \right). \tag{17}$$

We have found from LES of the neutral ABL that ξ_1 is typically ≈1.05. The ensemble mean of the eddy viscosity at the first grid level with the Smagorinsky closure is

$$\left\langle \nu_t \right\rangle_1 = C_s^2\Delta^2\left\langle (2s_{ij}^r s_{ij}^r)^{1/2} \right\rangle_1 \approx 2C_s^2\Delta^2\left\langle s_{13}^r \right\rangle_1 = C_s^2\Delta^2\left(\frac{\partial U}{\partial z} \right)_1 , \tag{18}$$

where

$$\left\langle (s_{ij}^r s_{ij}^r)^{1/2} \right\rangle_1 \approx \sqrt{2}\left\langle s_{13}^r \right\rangle_1 \left(1 + \frac{1}{8}\frac{\left\langle s_{ij}^{r\,\prime} s_{ij}^{r\,\prime} \right\rangle_1}{\left\langle s_{13}^r \right\rangle_1^2} \right)$$

is well approximated by $\sqrt{2}\left\langle s_{13}^r \right\rangle_1$ since the strain-rate fluctuations are nearly all subfilter-scale (this is especially true at the first grid level where the integral scales are minimally or poorly resolved). We write the mean streamwise velocity gradient in a form appropriate for inertial scaling in the surface layer[3]:

[3] When the Coriolis force is present, as in LES of the atmospheric boundary layer, the velocity at the first grid level is at an angle θ_1 to the geostrophic wind velocity above the boundary layer. In this case, equations (19), (20), (21), (23), (24), (27), (28) contain an additional factor $\cos\theta_1$, as given in Appendix A.

$$2\left\langle s_{13}^{r}\right\rangle_{1}=\left(\frac{\partial U}{\partial z}\right)_{1}\equiv\frac{u_{*}}{\tilde{\kappa}_{1}z_{1}}. \tag{19}$$

In Eq. (19) $\tilde{\kappa}_1$ is defined as the value required to make the LHS equal to the RHS at the first grid level. Only if LOTW is predicted by the LES, so that $\tilde{\kappa}_1$ is constant through the surface layer, will $\tilde{\kappa}_1$ be the predicted value of the von Kármán constant.

Inserting (19) into (18) and (17) leads to the following expression for the LES viscosity:

$$\nu_{LES}=\frac{\xi_1}{\tilde{\kappa}_1}D_s u_*\Delta_z \text{, where } D_s\equiv C_s^2 A_R^{\,4/3}. \qquad \text{(Smagorinsky)} \tag{20}$$

$A_R=\Delta_x/\Delta_z=\Delta_y/\Delta_z$ is the aspect ratio of the grid and $\Delta_z=z_1$ is the vertical grid spacing. As will be discussed at length, Eq. (20) indicates that the LES viscosity is proportional to the combination $C_s^2 A_R^{\,4/3}$, and therefore is altered both by the constant in the SFS model and by the aspect ratio of the grid, as well as by the vertical grid spacing.

Applying Kolmogorov scaling[38] and LOTW scaling to the one-equation model produces a result similar to Eq. (20), but with D_s replaced by $D_k=C_k A_R^{\,8/9}$ and with $\tilde{\kappa}_1$ replaced by a different order one constant, β. The main point is that with the eddy viscosity closure, the LES viscosity is proportional to the product of model constant and grid aspect ratio, each raised to a power that depends on the closure.

In order to develop an expression for $\Re$, we note that since the total shear stress is $T_{tot}=T_R+T_S$, $\Re$ is given by

$$\Re=\frac{T_{tot_1}}{T_{S_1}}-1=\frac{\xi_2(\rho u_*^2)}{T_{S_1}}-1, \qquad \text{(closure independent)} \tag{21}$$

where

$$\xi_2\equiv\frac{T_{tot_1}}{T_{tot_0}}\approx\frac{N_\delta-1}{N_\delta}. \tag{22}$$

In (21) and (22) $T_{tot_0}=\rho u_*^2$ and $N_\delta=\delta/\Delta_z$ is the number of grid points from the surface to the top of the boundary layer. ξ_2 is generally very close to 1.

Inserting Eq. (19) for $\left\langle s_{13}^{r}\right\rangle_1$ and Eq. (20) for ν_{LES} into $T_{S_1}=2\rho\nu_{LES}\left\langle s_{13}^{r}\right\rangle_1$, and then inserting this result for T_{S_1} into Eq. (21) produces the following expression for $\Re$:

$$\Re=\frac{\xi\beta\tilde{\kappa}_1}{D_t}-1, \qquad \text{(eddy viscosity)} \tag{23}$$

where $\xi\equiv\xi_2/\xi_1$ is generally very close to 1. For the Smagorinsky closure, $\beta=\tilde{\kappa}_1$ and $D_t\rightarrow D_s=C_s^2 A_R^{\,4/3}$, whereas for the one-equation model $D_t\rightarrow D_k=C_k A_R^{\,8/9}$ and β is a different order one constant.

The eddy viscosity closure was used in the derivation of Eq. (23) to provide insight into the mechanisms underlying $\Re$ and how it can be systematically adjusted in large-eddy simulation in order to move the LES into the supercritical regime $\Re>\Re^*$. We learn that the ratio of resolved to SFS stress at the first grid level can be increased either by reducing the model constant or by reducing the grid aspect ratio and that these two changes act in combination through:

$$D_t=C_t^a A_R^{\,b}, \tag{24}$$

where the model constant C_t (Eq. 15) and A_R enter in this combination through the LES viscosity, Eq. (20), and the powers *a* and b are model-dependent. Thus, LES viscosity can be decreased and $\Re$ increased by reducing either or both C_t and A_R to reduce D_t.

The explanation behind the effects of model constant and A_R on $\Re$ is in the manner that each reduction affects the balance between resolved and SFS stress within the total stress $T_{tot}(z)$ that is fixed by the global momentum balance. Reducing the model constant directly reduces the average SFS stress T_S. Reducing the aspect ratio corresponds to an increase in resolution in the horizontal, which moves vertical velocity variance and Reynolds stress from subfilter-scales to resolved scales in the horizontal. The consequence of both effects is to reduce T_S relative to T_R, and therefore to increase the ratio $\Re = T_{R_1} / T_{S_1}$. Similarly, both effects reduce LES viscosity.

III. The Balance between Numerical Friction and Inertia: a Second Observation

The above suggests that the mechanisms that underlie the generation of a mean gradient overshoot and its consequences are associated with *numerical LES friction* that, in the modeled dynamical system, forces a physical response similar to that underlying the overshoot in Newtonian turbulent channel flow (Fig. 3) that results from *molecular friction*. Correspondingly, like the real viscous layer in smooth wall channel flow that arises from a change in scaling from *z* to $\ell_\nu = \nu / u_*$, the overshoot in LES reflects a transition in dominance from the inertial surface scale *z* to a numerical LES viscous length scale $\ell_{\nu_{LES}} = \nu_{LES} / u_*$ that dominates near the surface. LES produces an overshoot in $\Phi_m(z)$ as a result of the spurious dominance of this length scale $\ell_{\nu_{LES}}$ in a region where the integral scales should scale on *z*.

However, for the LOTW to exist in an inertia-dominated surface layer, inertial effects must be sufficiently strong relative to viscous forces, as measured by the ratio of the boundary layer depth to the viscous wall scale, the Reynolds number $\mathrm{Re}_\tau = \delta / \ell_\nu$. This suggests the existence of a "LES Reynolds number," $\mathrm{Re}_{LES} = \delta / \ell_{\nu_{LES}}$. Since friction in the discretized LES dynamical system is at the core of the overshoot, we must consider all consequences of friction, including the requirement that inertial effects dominate viscous effects sufficiently to produce the LOTW scaling, $\partial U / \partial z \sim u_* / z$.

In particular, in the smooth wall channel flow the inertial layer will only reflect the LOTW when inertia dominates the viscous force within the surface layer sufficiently that Re_τ exceeds a critical value, Re_τ^*. The DNS data of Fig. 3 shows that the LOTW is not captured in the viscous channel flow even at $\mathrm{Re}_\tau = 2003$, when the viscous layer (defined by the peak in Φ_m) is only 2% of the surface layer.

Similarly, one can expect that LES of the high Reynolds number boundary layer can only produce LOTW scaling when inertia in the discretized dynamical system dominates friction sufficiently that the LES Reynolds number Re_{LES} exceeds some critical value, Re_{LES}^*. Indeed one can also postulate a transitional Re_{LES} which must be exceeded to support turbulence in the discretized LES dynamical system. In Fig. 5 we show four large-eddy simulations of the atmospheric boundary layer at increasing values of Re_{LES}. Similar to Fig. 3 for DNS of channel flow where the peak in the overshoot scales on the viscous scale ℓ_ν, with the exception of the lowest Re_{LES} (thin solid curve with small dots), the overshoot in LES scales on the numerical LES viscous scale, $\ell_{\nu_{LES}}$ (Fig. 5(a)). In fact, both the true channel-flow overshoot and the spurious LES overshoot peak at 10 corresponding viscous units. Thus, the LES overshoot moves closer to the surface along with $\ell_{\nu_{LES}}$ as $\mathrm{Re}_{LES} = \delta / \ell_{\nu_{LES}}$ increases (Fig. 5(c)) and the numerical LES viscous layer occupies a correspondingly smaller percentage of the surface layer. Similarly, the peak in $\Phi_m(z)$ coincides with the crossover between mean resolved and SFS stress T_R and T_S (Fig. 5d) so that the crossover also scales on $\ell_{\nu_{LES}}$ (Fig. 5(b)).

The thin solid curve (with small dots) in Fig. 5(c) is included to illustrate the consequence of a LES Reynolds number that is too low to support turbulence. The mean velocity profile is qualitatively similar to the parabolic profile characteristic of laminar Newtonian channel flow. Thus, although the LES equation contains no true frictional term, the numerical LES friction inherent in the model and adjusted by the grid as described by ν_{LES} in Eq. (20) can, like real friction, dampen inertial motions and prevent turbulence within the discretized dynamical system advanced in the LES.

The frictional content of the simulation embodied by ν_{LES} should, in principle, be extended to include the numerical dissipation within the specific discretization that is applied to advance the LES equations in time with a SFS model. The LES presented in Sect. VI apply the pseudo-spectral method in the horizontal and finite difference in the vertical on a staggered mesh and is minimally dissipative. Significant frictional content within the numerical algorithm might strengthen the overshoot beyond what is described here.

A. The second and third criteria

The first criterion discussed in Sec. III.C is a necessary condition to eliminate the overshoot but is not a sufficient condition to correctly predict LOTW scaling in the high Reynolds number surface layer—that is, constant $\phi(z)$ is the surface layer. A second criterion is necessary: that Re_{LES} exceed a critical Re^*_{LES} to achieve LOTW scaling in the simulated dynamical system. In the presence of the overshoot, one would expect that to predict the LOTW in the part of the surface layer that is not directly affected by numerical LES friction, Re^*_{LES} would have to achieve values in the thousands similar to Re^*_{τ} in real frictional channel flow. However, unlike DNS of channel flow where the overshoot is real and cannot be eliminated, in LES of high Reynolds number boundary layers the overshoot and its frictional sources are spurious. Therefore, the critical Reynolds number Re^*_{LES} required to satisfy the second criterion turns out to be much lower when $\Re > \Re^*$ (and the overshoot is eliminated) than when the overshoot is maintained as in Fig. 5.

To show this we use Eq. (19) to write:

$$T_{S_1} = 2\rho\nu_{LES}\left\langle s^r_{13}\right\rangle_1 = \rho\nu_{LES}\frac{u_*}{\tilde{\kappa}_1 z_1}. \qquad \text{(closure independent)} \qquad (25)$$

Inserting Eq. (25) into Eq. (21) yields an expression for Re_{LES} that is valid independent of the SFS model:

$$\mathrm{Re}_{LES} = \frac{N_\delta}{\xi_2\tilde{\kappa}_1}(\Re + 1). \qquad \text{(closure independent)} \qquad (26)$$

Thus Re_{LES} depends both on $\Re$ and on the vertical grid resolution N_δ. (Note that in Fig. 5(c) the LES give by the solid curve has low Re_{LES} because of low vertical grid resolution.) The critical LES Reynolds number Re^*_{LES} is therefore associated not only with the critical ratio of resolved to SFS stress $\Re^*$, but also with a critical vertical resolution, N^*_δ where

$$\mathrm{Re}^*_{LES} = \frac{N^*_\delta}{\xi_2\tilde{\kappa}_1}(\Re^* + 1). \qquad \text{(closure independent)} \qquad (27)$$

The third criterion, that N_δ exceed a critical value N^*_δ, follows from the second criterion, $\mathrm{Re}_{LES} > \mathrm{Re}^*_{LES}$ when $\Re \geq \Re^*$.

One way to understand the requirement for a minimum vertical resolution to produce high accuracy LES of the boundary layer is simply as a manifestation of the standard computational requirement that all special regions with their own characteristic dynamics be well resolved for accurate numerical simulation. The surface layer is an example of a region with special dynamics that requires good resolution. The

surface layer occupies ~15-20% of the boundary layer depth at high Reynolds numbers. Resolving this layer with, say, 10 grid points in the vertical therefore leads to an estimate for N_δ^* of ~50-65. Recognizing that $\Re^*$ and Re_{LES}^* are model-dependent, we can estimate Re_{LES}^* roughly for $\Re^* \approx 1$ to be $\mathrm{Re}_{LES}^* \sim 250-325$. This estimate assumes that the overshoot has been eliminated and that the LOTW has been captured with $\tilde{\kappa}_1 = \kappa \approx 0.4$. That is, we assume that there are no additional confounding influences that cause the LES to deviate from the LOTW. (In Sect. VII we shall discuss confounding influences.) This estimate for Re_{LES}^* is well over an order of magnitude *lower* than what we would estimate by analogy with Re_τ^* in DNS of channel flow if the overshoot were retained, but confined to a sufficiently thin, numerically viscous, layer adjacent to the surface.

We shall find (Sect. VI) that, for our current LES of the ABL with the Smagorinsky eddy viscosity closure, 45-50 is a reasonable estimate for N_δ^* and 350 is a reasonable estimate for Re_{LES}^*. The good news is that a vertical grid resolution $N_z \approx 2N_\delta^* \sim 90-100$ is not overly severe and doable on current mainframes. The bad news is that most calculations in the literature are of LES with vertical resolutions below critical. Interestingly, we shall show in Sect. V.B that, in addition to subcritical resolution in the vertical, there are practical limitations to the maximum vertical resolution in LES of the high Reynolds number boundary layer.

B. Understanding the LES Reynolds number and the three criteria

To develop greater insight into the LES Reynolds number and its control, we evaluate $\mathrm{Re}_{LES} = \delta / \ell_{\nu_{LES}}$ using the Smagorinsky eddy viscosity representation for the SFS stress as was done to understand $\Re$ in Sect. III.D. There we derived an expression for the LES viscosity, ν_{LES} (Eq. 20). Using this expression, the numerical LES viscous length scale is given by:

$$\ell_{\nu_{LES}} \equiv \frac{\nu_{LES}}{u_*} = \frac{\xi_1}{\beta} D_t \Delta_z, \qquad \text{(eddy viscosity)} \qquad (28)$$

where $\beta = \tilde{\kappa}_1$ for the Smagorinsky closure. Dividing δ by Eq. (28), or replacing $\Re$ in Eq. (26) by Eq. (23), produces the following expression for the LES Reynolds number:

$$\mathrm{Re}_{LES} = \frac{\beta}{\xi_1} \frac{N_\delta}{D_t}. \qquad \text{(eddy viscosity)} \qquad (29)$$

Several interesting observations can be extracted from Eqs. (28) and (29). Since the overshoot scales on $\ell_{\nu_{LES}}$ and peaks at $10\,\ell_{\nu_{LES}}$ (Fig. 5), the observation made in Sect. II.C from previous studies—that the overshoot is tied to the grid—can now be explained. Equation (28) shows that if neither the model constant nor the grid aspect ratio are altered while the grid is refined, the LES viscous scale $\ell_{\nu_{LES}}$, and therefore the peak in Φ_m, will move closer to the surface in proportion to the grid spacing, Δ_z. However, since $D_t = C_t^a A_R^{\ b}$ is left unchanged during the grid refinement, $\Re$ and the magnitude of the overshoot will not change—the overshoot simply moves closer to the surface as shown in Figs. 3 and 5. In particular, Fig. 5 shows that as the overshoot moves towards the surface in proportion with the grid spacing at constant A_R and C_t, the ratio $T_{R_1} / T_{S_1} = \Re$ and magnitude of peak Φ_m remain unchanged and the locations of peak Φ_m remains attached to the crossover between T_R and T_S.

A second interpretation follows by replacing Re_{LES}^* with $\delta / \ell_{\nu_{LES}}^*$ in Eq. (27). The criterion $\Re > \Re^* \approx 1$ is then equivalent to:

$$\frac{\ell_{\nu_{LES}}}{\Delta_z} < \frac{\ell^*_{\nu_{LES}}}{\Delta_z} = \frac{\xi_2 \tilde{\kappa}_1}{\Re^* + 1} \sim 0.2 . \qquad \text{(closure independent)} \qquad (30)$$

Equation (30) states that the spurious length scale $\ell_{\nu_{LES}}$ arising from friction within the SFS model and grid under-resolution in a large-eddy simulation must be confined sufficiently well within the first grid cell for numerical LES friction to not adversely affect the LES. Note that Eq. (30) is equivalent to the requirement that $z^+_{1_{LES}} \gtrsim 5$: the first grid level must be at least five times than the spurious viscous length scale.

The inequality (30) is satisfied when $\Re > \Re^*$, so that the first and second criteria are met when the spurious viscous length scale is sufficiently small relative to the grid spacing. However (30) does not guarantee the third criterion, $N_\delta > N^*_\delta$. This is because the overshoot peaks at $10\,\ell_{\nu_{LES}}$, so that the condition given by (30) still allows partial resolution of the overshoot (e.g., when $10\ell_{\nu_{LES}}/\Delta_z \sim 2$). One can therefore interpret the addition of the third criterion, $N_\delta > N^*_\delta$, as demanding that the spurious frictional length scale $\ell_{\nu_{LES}}$ be buried both sufficiently far within the first grid level Δ_z and within the boundary layer δ that the grid is given no opportunity to either create an overshoot or alter LOTW scaling through the influence of friction within the surface layer.

IV. A Framework for High-Accuracy Large-Eddy Simulation: the "High-Accuracy Zone"

By comparing Eq. (23) for $\Re$ with Eq. (29) for Re_{LES} we learn that reducing the model constant and/or the grid aspect ratio in the combination $D_t = C_t^a A_R^{\,b}$ causes both $\Re$ and Re_{LES} to increase (and, correspondingly, $\ell_{\nu_{LES}}/\Delta_z$ to decrease). However, increasing only the vertical resolution increases the LES Reynolds number but has no effect on the ratio of resolved to SFS stress, $\Re$. This observation leads to the concept of a "$\Re - \mathrm{Re}_{LES}$ parameter space" in which high-accuracy LES of the high Reynolds number boundary layer could be developed. Within this framework, one can systematically adjust LES of the boundary layer so that, in the high Reynolds number limit, the overshoot is suppressed and the LOTW is captured. The $\Re - \mathrm{Re}_{LES}$ parameter space is illustrated in Fig. 6; a large-eddy simulation of the boundary layer is identified as a point on a plot of $\Re$ against Re_{LES}. In subsequent simulations, the LES is adjusted to move the point within the $\Re - \mathrm{Re}_{LES}$ parameter space relative to the critical parameters $\Re^*$, Re^*_{LES} and N^*_δ.

For the LES to capture the LOTW while resolving the overshoot, the simulation must live in the rectangular space $\Re > \Re^*$, $\mathrm{Re}_{LES} > \mathrm{Re}^*_{LES}$. We have roughly estimated $\Re^* \sim 1$ and $\mathrm{Re}^*_{LES} \sim 350$. However in addition to the criteria $\Re > \Re^*$ and $\mathrm{Re}_{LES} > \mathrm{Re}^*_{LES}$, we have argued for a third criterion, $N_\delta > N^*_\delta$. $\Re$ and Re_{LES} are linearly related by Eq. (26):

$$\Re = \left(\frac{\xi_2 \tilde{\kappa}_1}{N_\delta} \right) \mathrm{Re}_{LES} - 1 . \qquad \text{(closure independent)} \qquad (31)$$

Thus, N_δ enters in the slope of $\Re$ vs. Re_{LES}. In Fig. 6 we plot Eq. (31) as a series of lines with constant slope $\xi_2 \tilde{\kappa}_1 / N_\delta$. Since LOTW is only captured in the supercritical region of the $\Re - \mathrm{Re}_{LES}$ parameter space, in general $\tilde{\kappa}_1$ will vary from point to point on lines of constant slope $\xi_2 \tilde{\kappa}_1 / N_\delta$. However the variation in $\tilde{\kappa}_1$ is not so great as to obscure the strong inverse relationship between the slopes of the $\Re - \mathrm{Re}_{LES}$ lines and the vertical grid resolution N_δ. It can be shown from Eq. (27) that the third criterion,

$N_\delta > N_\delta^*$, is met when the simulation lies to the right of the $\Re - \mathrm{Re}_{LES}$ line with slope $\xi_2 \tilde{\kappa}_1 / N_\delta^*$ that passes through the intersection between $\Re = \Re^*$ and $\mathrm{Re}_{LES} = \mathrm{Re}_{LES}^*$, as illustrated in Fig. 6. We call the wedge-shaped region that defines supercritical LES satisfying all three criteria $\Re > \Re^*$, $\mathrm{Re}_{LES} > \mathrm{Re}_{LES}^*$, and $N_\delta > N_\delta^*$ the "High-Accuracy Zone," or HAZ. The LES must reside within the HAZ to meet the three criteria required to both eliminate the overshoot and capture the LOTW.

A. Designing LES to capture law-of-the-wall scaling

The objective is to systematically move the large-eddy simulation into the HAZ of the $\Re - \mathrm{Re}_{LES}$ parameter space by combining Eq. (31) with knowledge gained from Eqs. (23) and (29). Although we have applied eddy viscosity closures to gain insight into the process of adjusting N_δ, $\Re$ and Re_{LES} to systematically move the LES within the $\Re - \mathrm{Re}_{LES}$ parameter space, the basic method can be applied with any SFS stress model. T_{R_1} and T_{S_1} (and therefore $\Re$), and ν_{LES} (and therefore Re_{LES}) can be quantified independent of SFS model, the only requirement being that all contributions to the SFS stress are included in defining τ_{ij}^{SFS} before calculating T_{S_1}. This relatively simple process may be described in two basic steps:

1. Adjust, and hold fixed, the vertical resolution of the grid (N_z) so that when the simulation is fully developed, N_δ will exceed N_δ^* (typically, $N_z \sim 1.5N_\delta - 2N_\delta$ to minimize the influence of the upper boundary condition). We shall point out in the next section that it is possible to *over* resolve in the vertical.
2. Then systematically adjust the aspect ratio of the grid together with the model constant to move the simulation roughly along a straight line in Fig. 6 from the subcritical region of the $\Re - \mathrm{Re}_{LES}$ parameter space into the HAZ. With eddy viscosity closures, the model constant and aspect ratio appear in the combination $D_t = C_t^a A_R^{\ b}$. However to move into the HAZ with any other closure, one would adjust the model constant for that closure (to systematically reduce the SFS stress) together with a systematic increase the horizontal resolution of the grid (to systematically reduce the aspect ratio).

We presume that the closure for SFS stress relies on a dissipative mechanism to model the net transfer of resolved turbulence energy to subfilter scale motions. With this methodology for designing LES one can analyze systematically what works better or worse depending on choice of model type, model details, model constant, grid resolution, grid structure, algorithm, geometry, etc., with some understanding of underlying mechanisms. This framework provides the LES community with both physical understanding and structure upon which a systematic procedure for LES design may be based. Once the researcher has become experienced with the method, s/he will be able to design high-accuracy LES more rapidly using her/his favorite SFS model, algorithm, code, etc.

Whereas the model constant C_t and the model length scale $\ell_t = C_t \Delta$ are uniform in the above discussions, in the general eddy viscosity model the length scale ℓ_t is specified as varying with z. The Mason & Thomson[1] modification of the length scale ℓ_t near the surface and the dynamic procedure that adjusts the Smagorinsky constant C_s with z (e.g., Porté-Agel *et al.*[25]) are examples. The primary issue is that the level of eddy viscosity be adjusted in concert with the grid aspect ratio (i.e., the horizontal resolution of vertical motions) within the first few grid levels from the surface, where under-resolution is of primary concern and mean SFS stress competes with resolved stress.

B. Grid-independent LES and practical limits on grid resolution

As discussed in Sect. II.C, a problem with current LES of the ABL is grid dependence in the mean flow. We shall show in the next section that as the simulation moves systematically into the HAZ within the $\Re - \mathrm{Re}_{LES}$ parameter space, a grid-independent solution for the mean velocity is achieved. However,

one cannot move the simulation infinitely far into the HAZ along lines of fixed vertical grid resolution N_δ, since that would require that either the model constant be driven to zero (removing the model from the dynamical system) or the grid aspect ratio would be taken to zero (creating infinitesimally thin grid cells and infinite computational expense). Either of these limits will cause numerical problems and simulation error regardless of computational expense. Thus, for both accuracy and practical reasons, the optimal location for the simulation within the HAZ is near the apex of the wedge in Fig. 6 where $\mathfrak{R} \gtrsim \mathfrak{R}^*$, $\mathrm{Re}_{LES} \gtrsim \mathrm{Re}^*_{LES}$, and $N_\delta \gtrsim N^*_\delta$.

Similarly there are practical limits on vertical resolution that, surprisingly, confine the growth of LES grids on any given computer. Although a minimum vertical resolution is required to move the simulation into the HAZ, progressive increases in vertical resolution will force the simulation onto lines in the $\mathfrak{R} - \mathrm{Re}_{LES}$ parameter space that have progressively smaller slopes, as illustrated by the dashed line in Fig. 6. Increases in vertical grid resolution in the absence of other adjustments will increase grid aspect ratio, driving $\mathfrak{R}$ to sub critical values and restoring the overshoot along with its related errors. With eddy viscosity models, for example, in order that $\mathfrak{R} \approx \mathfrak{R}^*$ as N_δ is increased, $D_t = C_t^a A_R^b$ must be held constant (Eq. 23). However, since the minimum model constant and maximum grid aspect ratio are bounded, grid aspect ratio must, at some point, be maintained roughly fixed with increasing vertical resolution, and horizontal grid resolution must increase proportionally with N_δ. The number of grid points will therefore increase approximately as N_δ^3, severely limiting the vertical resolution to modest values. This dilemma is reminiscent of direct numerical simulation where the highest Reynolds number that can be simulated accurately grows slowly with increasing computer size due to the rapid increase in resolution requirements with increasing Reynolds number.

V. Numerical Experiments

To evaluate the theory and further explore the application of the $\mathfrak{R} - \mathrm{Re}_{LES}$ framework to the development of wall bounded LES, we have carried out over 110 large-eddy simulations of the neutral shear-driven atmospheric boundary layer capped with an inversion layer to suppress boundary layer growth and produce a quasi-stationary long-time solution. The Coriolis force is included at a relatively high level to reduce the time to reach quasi stationary, so the mean wind is skewed relative to the geostrophic wind (*x* direction) at the first grid level (see Appendix A). The code is pseudo-spectral in the horizontal and finite difference in the vertical, so numerical dissipation is minimal. In the horizontal statistically homogeneous directions we apply periodic boundary conditions; in the vertical we apply the boundary conditions as described in Moeng[37] and Sullivan *et al.*[39]. We report here on simulations with the Smagorinsky closure and uniform grid spacing. In particular, we apply the nonlinear Moeng[37] model for total fluctuating shear stress at the lower surface and the friction velocity is made proportional to the mean wind at the first grid level with a proportionality constant that can be related to the surface roughness length scale, z_0. A summary of the numerical algorithm and simulations is given in Appendix B and in several publications[37,11,39,18].

It should be noted that, in our code, dealiasing in the horizontal directions is carried out by padding rather than truncation. These are equivalent except in the interpretation of the grid and grid length scale: the grid resolutions and aspect ratios quoted in the figures are *before* padding and the grid length scale $\Delta = (\Delta_x \Delta_y \Delta_z)^{1/3}$ used in the in the eddy viscosity model (Eq. 15) is also based on the pre-padded grid. In all plots we define the boundary layer thickness δ at the height where the mean velocity gradient crosses zero. Whereas the number of grid points in the vertical, N_z, is defined before the simulation, the number of grid points within the boundary layer, N_δ, is determined after a simulation is analyzed in the quasi-stationary state. We were careful to determine the quasi-stationary state consistently in all simulations (see Appendix B). In all plots of $\Phi_m(z) = \kappa\phi(z)$ we use a value of 0.40 for κ.

A. The $\Re - \mathrm{Re}_{LES}$ parameter space

In Fig. 7 we identify in the $\Re - \mathrm{Re}_{LES}$ parameter space all the simulations carried out for the current study. As will be discussed below, from the predictions of $\Phi_m(z)$ we estimated the critical lines $\Re = \Re^*$, $\mathrm{Re}_{LES} = \mathrm{Re}_{LES}^*$, and $N_\delta = N_\delta^*$ drawn on the figures. In Fig. 7(a) different symbols are used according to the number of grid points in the vertical, N_z ($\approx 1.5\,N_\delta$). These show approximate correspondence to the straight line representations of Eq. (31) in Fig. 6 at constant slope, $(\xi_2\tilde{\kappa}_1 / N_\delta)$. Note that the points in Fig. 7(a) become noticeably more linear as the simulations enter the triangular HAZ region of the $\Re - \mathrm{Re}_{LES}$ parameter space and $\tilde{\kappa}_1$ better represents the von Kármán constant. To demonstrate, as per Eq. (23), that $\Re$ increases with decreasing $D_s = C_s^2 A_R^{4/3}$, in Fig. 7(b) different symbols are used according to $C_s^2 A_R^{4/3}$ creating horizontal bands of distinct symbol type consistent with increasing $\Re$. Note that the bands also shift to higher Re_{LES} with increasing $\Re$ and $C_s^2 A_R^{4/3}$ as per Eqs. (26) and (29).

B. The "High Accuracy Zone" (HAZ)

To show the transition from subcritical regions of the $\Re - \mathrm{Re}_{LES}$ parameter space to the supercritical HAZ, consider the 16 simulations on the four paths shown in Fig. 8 with the point symbols. Each path has fixed vertical resolution, N_z, and progresses from lower to higher $\Re$ and Re_{LES} along lines of constant N_z, roughly lines of constant slope $(\xi_2\tilde{\kappa}_1 / N_\delta)$ in Eq. (31).

In Fig. 9 we plot $\Phi_m(z)$ against z/δ for each of the groups of 4 simulations at fixed N_z in Fig. 8. In Sect. IV.A we argued for the existence of a critical vertical resolution N_δ^* below which the surface layer is insufficiently resolved and the LOTW can therefore not be properly captured. The four groups of curves in Fig. 9 show the consequences of poor resolution of the surface layer in the vertical and provides an estimate for N_δ^*. In Fig. 9(a) the surface layer is resolved with, at best, 3 grid points. This clearly insufficient vertical resolution is associated with $\Phi_m(z)$ curves that incorrectly bend to the left from the surface with increasing z; this occurs even when $\Re$ exceeds 1. Furthermore, the under-resolution of the surface layer in the vertical affects the mean velocity gradient and mean velocity profiles throughout the boundary layer; the mean gradient decreases too rapidly in z. It is not until Fig. 9(c), N_z = 96, that this spurious drop in Φ_m with z transitions to the profile $\Phi_m(z)$ extending vertically from the surface as is required by LOTW. The number of grid points in the surface layer (up to z/δ = 0.2) is 8- 9, suggesting that this is the critical resolution for the surface layer and that N_δ^* for these large-eddy simulations is ~ 40-45. We have drawn a line at constant slope $\kappa / N_\delta^* = 0.4/45$ in Figs. 7 and 8 showing how paths (a) and (b) remain outside the HAZ and paths (c) and (d) enter the HAZ at higher $\Re$ and Re_{LES}.

By comparing the groups of Φ_m curves (c) and (d) in Fig. 9, we note that as the simulations progress to higher $\Re$ and Re_{LES} along lines of constant N_z, in both groups the final two curves approach grid independence and the LOTW is captured as the overshoot is suppressed. To study the transition in the surface layer in detail, and to estimate $\Re^*$ and Re_{LES}^*, we compare the six simulations shown in Fig. 8 with the open circles which lie along each of the two paths, N_z = 96 and N_z = 128. The variations in $\Phi_m(z)$ in the lower 40% of the boundary layer for each point along the two paths are shown separately in Fig. 10. Comparing the upper and lower sets of figures, we observe nearly identical transitions along each of the two paths into the HAZ. At the lowest $\Re$ and Re_{LES} an overshoot obscures the surface layer and LOTW is not predicted by the LES. As $\Re$ and Re_{LES} increase (by decreasing $C_s^2 A_R^{4/3}$), the same

transition in $\phi(z)$ takes place along each path: the overshoot progressively decreases and a region of constant $\Phi_m(z)$ progressively strengthens until a well-defined region of constant $\Phi_m(z)$ appears in the surface layer that is maintained when $\Re^*$ and Re^*_{LES} exceed about 0.85 and 350, respectively, using the Smagorinsky closure. (The oscillations near the surface will be discussed in the next section.) The estimates for the lines that define the HAZ from the critical Smagorinsky model parameters $\Re^* \approx 0.85$, $\mathrm{Re}^*_{LES} \approx 350$, and $N^*_\delta \approx 45$ are drawn in figures 7, 8, and 11(a).

Figure 10 shows that as N_z, C_s and A_R are adjusted so as to progressively move the large-eddy simulation from the subcritical part of the parameter space into the High-Accuracy Zone, the mean velocity gradient approaches a fixed point independent of the path taken into the HAZ. In Fig. 11 we plot normalized mean velocity gradient distributions for five of our computed large-eddy simulations within the HAZ at different vertical grid resolutions N_δ and combinations, $C_s^2 A_R^{4/3}$. Fig. 11(a) shows the locations of these five simulations on the $\Re - \mathrm{Re}_{LES}$ parameter space (all but the + symbol). Fig. 11(b) shows that these simulations within the HAZ are approximately grid-independent over the boundary layer depth. In Fig. 11(c) we expand the surface layer to show how the overshoot is suppressed and the LOTW is captured by the simulation (all but the dashed line).

In Fig. 7(a) we also show simulations from the literature. All but the simulation by Drobinski *et al.*[32] are well outside the HAZ. In two simulations, one from Andren *et al.*[10] and one from Porté-Agel *et al.*[25], $\Re$ was sufficiently high to remove the overshoot but the vertical resolution of the grid was insufficient for the LES to produce LOTW scaling.

In Fig. 11(a) the Drobinski *et al.*[32] simulation is indicated with the plus symbol and in Fig. 11(c) with the dashed line. Drobinski *et al.*[32] used a different numerical algorithm, a one-equation eddy viscosity model. Their model for surface shear stress was not indicated. Whereas their critical parameters $\Re^*$ and Re^*_{LES} are not necessarily the same (since they used a different SFS stress closure), their simulation appears to be well within the HAZ (Fig. 11a), their overshoot is suppressed and they have captured LOTW scaling (Fig. 11c). The Drobinski *et al.*[32] simulation predicts a different numerical value for $\phi(z)$ in the surface layer than do our simulations with the classical Smagorinsky closure and Moeng[37] surface stress model. Whereas the Smagorinsky model simulations in Fig. 11 predicted a von Kármán constant $\kappa \approx 0.33$, the Drobinski *et al.*[32] simulation produces a $\kappa \approx 0.35$. Factors that affect the prediction of the von Kármán constant are discussed in section VII.C.

It turns out that the von Kármán constant issue is associated with the development of oscillations in $\Phi_m(z)$ at grid cells adjacent to the surface (Fig. 10). The oscillations grow as the simulations move farther into the HAZ along a line of constant N_z. As will be discussed in Sect. VII, the oscillations originate in the spurious nature of the lower boundary condition for fluctuating surface shear stress. This observation is interesting, in part, because it has been previously reported that LES of the ABL is insensitive to the details of the lower stress boundary condition[11,40]. These simulations, however, were outside the HAZ and in the presence of the overshoot and its frictional source.

References

[1]P. J. Mason and D. J. Thomson, "Stochastic backscatter in large-eddy simulations of boundary layers," J. Fluid Mech. **242**, 51 (1992).

[2]H. M. Nagib and K. A. Chauhan, "Variations of von Kármán coefficient in canonical flows," Phys. Fluids 20, 101518 (2008).

[3]E. L. Andreas, K. L. Claffey, R. E. Jordan, C. W. Fairall, P. S. Guest, P. O. G. Persson, and A. A. Grachev, "Evaluation of the von Kármán constant in the atmospheric surface layer," J. Fluid Mech. **559**, 117 (2006).

[4]R. J. Francey and J. R. Garratt, "Interpretation of flux-profile observations at ITCE (1976)". J. Appl. Met. **20**, 603 (1981),

[5]U. Högström, "Review of some basic characteristics of the atmospheric surface layer," Boundary-Layer Met. **78**, 215 (1996).

[6]J. A. Businger, J. C. Wyngaard, Y. Izumi, and E. F. Bradley, "Flux-profile relationships in the atmospheric surface layer," J. Atmos. Sci. **28**, 181 (1971).

[7]J. C. Wyngaard, J. A. Businger, J. C. Kaimal, and S. E. Larsen, "Comments on 'A revaluation of the Kansas mast influence on measurements of stress and cup anemometer overspeeding'," Boundary-Layer Met. **22**, 245 (1982).

[8]J. W. Telford and J. A. Businger, "Comment on Von Kármán's constant in atmospheric boundary layer flow: reevaluated," J. Atmos. Sci. **43**, 2127 (1986).

[9]S. P. Oncley, C. A. Friehe, J. C. Larue, J. A. Businger, E. C. Itsweire, and S. S. Chang, "Surface-layer fluxes, profiles, and turbulence measurements over uniform terrain under near-neutral conditions," J. Atmos. Sci. **53**, 1029 (1996),

[10]A. Andren, A. R. Brown, J. Graf, P. J. Mason, C.-H. Moeng, F. T. M. Nieuwstadt, and U. Schumann, "Large-eddy simulation of a neutrally stratified boundary layer: A comparison of four computer codes," Q. J. R. Meteorol. Soc. **120**, 1457 (1994).

[11]P. P. Sullivan, J. C. McWilliams, and C.-H. Moeng, "A subgrid-scale model for large eddy simulation of planetary boundary-layer flows," Boundary-Layer Meteorol. **71**, 247 (1994).

[12]Wyngaard, J. C. 2004 Toward numerical modeling in the "Terra Incognita." J. Atmos. Sci. **61**, 1816-1826.

[13]P. R. Spalart, W. H. Jou, M. Strelets, and S. R. Allmaras, "Comments on the feasibility of LES for wings and on a hybrid RANS/LES approach," In C Liu, Z Liu (Eds.) *Advances in DNS/LES*, Greyden, Columbus, OH, 137 (1997)

[14]N. V. Nikitin, ,F. Nicoud, B. Wasistho, K. D. Squires, and P. R. Spalart, "An approach to wall modeling in large-eddy simulation," Phys Fluids **12**, 1629 (2000).

[15]P. R. Spalart, "Detached-Eddy Simulation," Annu. Rev. Fluid Mech. **41**, 181 (2009).

[16]U. Piomelli, E. Balaras, "Wall-layer models for large-eddy simulations." Annu. Rev. Fluid Mech. **34**, 349 (2002).

[17]S. Khanna, and J. G. Brasseur, "Three-dimensional buoyancy- and shear-induced local structure of the atmospheric boundary layer," J. Atmos. Sci. **55**, 710 (1998).

[18]S. Khanna and J. G. Brasseur, "Analysis of Monin-Obukhov similarity from large-eddy simulation," J. Fluid Mech. **345**, 251 (1997).

[19]M. A. LeMone, "The structure and dynamics of horizontal roll vortices in the planetary boundary layer." J. Atmos. Sci. **30**, 1077 (1973).

[20]N. Hutchins and I. Marusic, "Evidence of very long meandering structures in the logarithmic region of turbulent boundary layers," J. Fluid Mech. **579**, 1 (2007).

[21]A. Juneja and J. G. Brasseur, "Characteristics of subgrid-resolved-scale dynamics in anisotropic turbulence, with application to rough-wall boundary layers," Phys. Fluids. **11**, 3054, (1999).

[22]F. Ding, S. P. Arya, and Y.-L. Lin, "Large-eddy simulation of the atmospheric boundary layer using a new subgrid-scale model," Environ. Fluid Mech. **1**, 29 (2001).

[23]E. Leveque, F. Toschi, L. Shao, and J.-P. Bertoglio, "Shear-improved Smagorinsky model for large-eddy simulation of wall-bounded turbulent flows.: J. Fluid Mech. **570**, 491 (2007).

[24]B. Kosovic, "Subgrid-scale modeling for the large-eddy simulation of high-Reynolds-number boundary layers," J. Fluid Mech. **336**, 151 (1997).

[25]F. Porté-Agel, C. Meneveau, and M. B. Parlange, "A scale-dependent dynamic model for large-eddy simulation: application to a neutral atmospheric boundary layer," J. Fluid Mech. **415**, 261 (2000).

[26]I. Esau, "Simulation of Ekman boundary layers by large eddy model with dynamic mixed subfilter closure," Environmental Fluid Mech. **4**, 273 (2004).

[27]F. K. Chow, R. Street, M. Xue, and J. H. Ferziger, "Explicit filtering and reconstruction turbulence modeling for large-eddy simulation of neutral boundary layer flow," J. Atmos. Sci. **62**, 2058 (2005).

[28]V. C. Wong and D. K. Lilly, "A comparison of two dynamic subgrid closure methods for turbulent thermal-convection," Phys. Fluids **6**, 1016 (1994).

[29]Y. Zhou, J. G. Brasseur, and A. Juneja, "A resolvable subfilter-scale model specific to large-eddy simulation of under-resolved turbulence,: Phys. Fluids **13**, 2602 (2001).

[30]S. Stolz, N. A. Adams, and L. Kleiser, "The approximate deconvolution model for large-eddy simulations of incompressible flows," Phys. Fluids. **13**, 997 (2001).

[31]A. R. Brown, J. M. Hobson, and N. Wood, "Large-eddy simulation of neutral turbulent flow over rough sinusoidal ridges," Boundary-Layer Meteorol. **98**, 411 (2001).

[32]P. Drobinski, P. Carlotti, J-L. Redelsperger, R. M. Banta, V. Masson, and R. K. Newsom, Numerical and experimental investigation of the neutral atmospheric surface layer," J. Atmos. Sci. **64**, 137 (2007).

[33]P. J. Mason, "Large-eddy simulation: A critical review of the technique," Q. J. R. Meteorol. Soc. **120**, 1 (1994).

[34]K. Iwamoto, Y. Suzuki, and N. Kasagi, "Reynolds Number Effect on Wall Turbulence: Toward Effective Feedback Control," Int. J. Heat and Fluid Flow. **23**, 678 (2002).

[35]K. Iwamoto, "Database of Fully Developed Channel Flow," THTLAB Internal Report, No. ILR-0201. THTLAB, Dept. of Mech. Eng., The Univ. of Tokyo, (2002).

[36]S. Hoyas and J. Jimenez, "Scaling of the velocity fluctuations in turbulent channels up to $\mathrm{Re}_\tau = 2003$," Phys. Fluids **18**, 011702-1 (2006).

[37]C.-H. Moeng, "A large-eddy-simulation model for the study of planetary boundary layer turbulence," J. Atmos. Sci. **13**, 2052 (1984).

[38]G. K. Batchelor, *The Theory of Homogeneous Turbulence*, Cambridge University Press, Cambridge, U. K. (1953).

[39]P. P. Sullivan, J. C. McWilliams, and C.-H. Moeng, "A grid nesting method for large-eddy simulation of planetary boundary-layer flows" Boundary-Layer Meteorol. **80**, 167 (1996).

[40]J. C. Wyngaard, L. J. Peltier, and S. Khanna, "LES in the surface layer: surface fluxes, scaling, and SGS modeling," J. Atmos. Sci. **55**, 1733 (1998).

[41]S. C. Hatlee, J. C. Wyngaard, "Improved Subfilter-Scale Models from the HATS Field Data," J.Atmos. Sci. **64**, 1694 (2007).

[42]K. R. Sreenivasan, "An update on the energy dissipation rate in isotropic turbulence," Phys. Fluids **10**, 528 (1998).

[43]M. J. Otte, *Turbulent structure of the interfacial layer capping the atmospheric boundary layer*, Ph.D. Thesis, Dept. of Meteorology, The Pennsylvania State University (2002).

[44]U. Schumann, "Subgrid-scale model for finite difference simulation of turbulent flows in plane channels and annuli," J. Comput. Phys. **18**, 376 (1975).

[45]J. G. Brasseur, T. Wei, S. Ramachandran, "Predicting law-of-the-wall with LES: role of SFS and surface stress models," Bull. Amer. Phys. Soc. **54** (19), 228, (2009).

[46]R. D. Moser, N. P. Malaya, H. Chang, P.S. Zandonade, P. Vedula, A. Bhattacharya, A. Haselbacher, "Theoretically based optimal large-eddy simulation," Phys. Fluids **21**, 105104-1 - 105104-19, (2009).

[47]Y. Zhou, J. G. Brasseur, A. Juneja, "A resolvable subfilter-scale model specific to large-eddy simulation of under-resolved turbulence," Phys. Fluids **13**, 2601-2610 (2001).

[48]J. Bardina, J. H. Ferziger, and W. C. Reynolds, "Improved subgrid-scale models for large-eddy simulation," AIAA Paper 80, 1357 (1980).

[49]C. Meneveau, J. Katz, "Scale-invariance and turbulence models for large-eddy simulation," Ann Rev Fluid Mech **32**, 1–32 (2000).

[50]J. G. Brasseur, Y. Zhou, "A resolvable subfilter-scale model specific to large-eddy simulation of near-wall turbulence." *Bull. Amer. Phys. Soc.* **45** (9): 82 (2000).

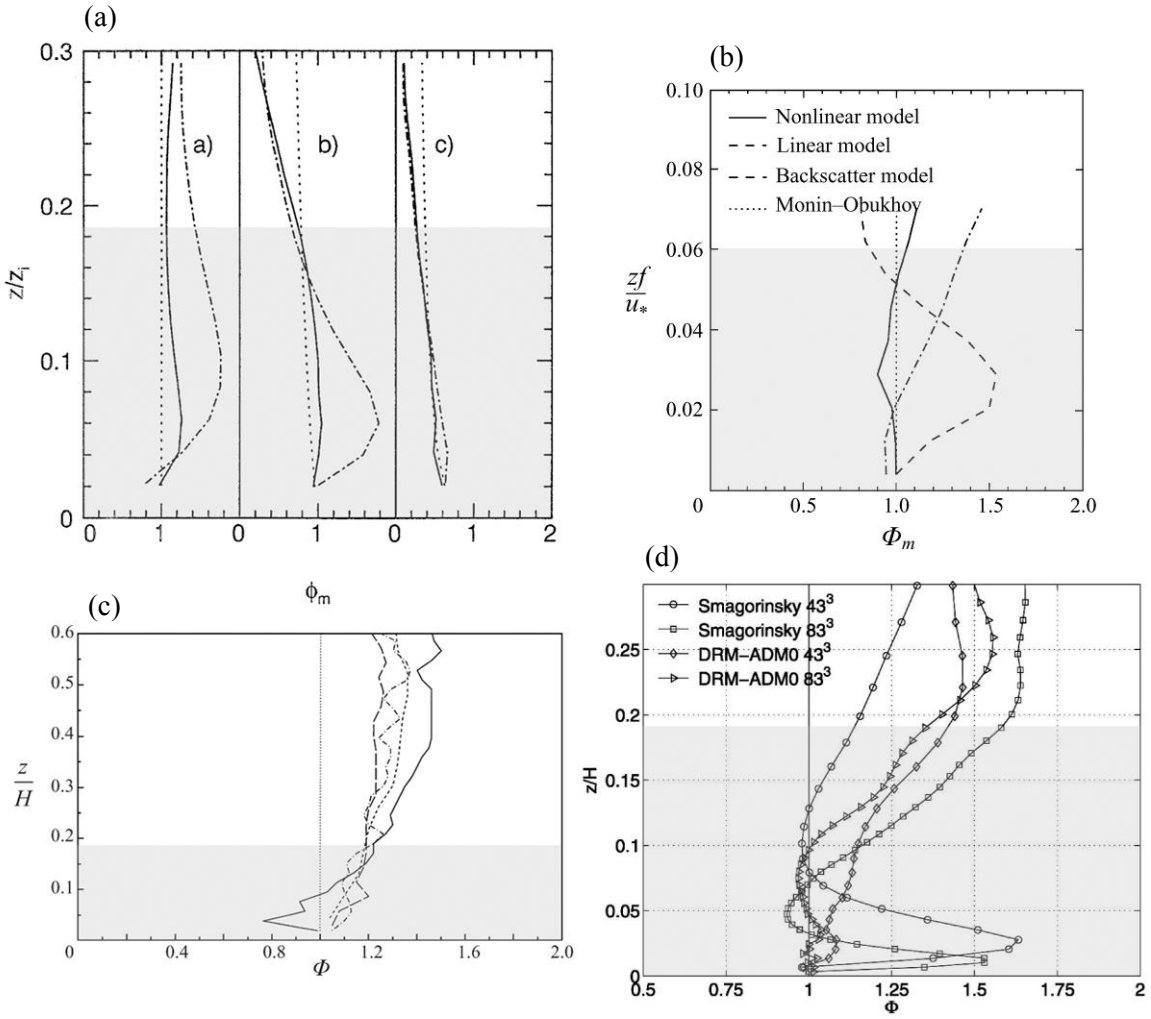

FIG. 1. Examples of the overshoot in mean shear from previous LES studies: (a) Sullivan *et al.*[11]. (b) Kosovic[24]. (c) Porté-Agel *et al*[25], and (d) Chow *et al.*[27]. In (a) z_i is the ABL depth defined in the traditional manner as the height where vertical turbulent heat flux is a minimum. In (b) z is scaled on u_*/f, where f is the Coriolis parameter (the angular velocity at the earth's surface). The simulations in (c) and (d) are pseudo-ABL/channel-flow simulations which do not contain a capping inversion and instead apply fixed horizontal velocity at $z = H$. $\kappa = 0.4$ was assumed in forming Φ_m.

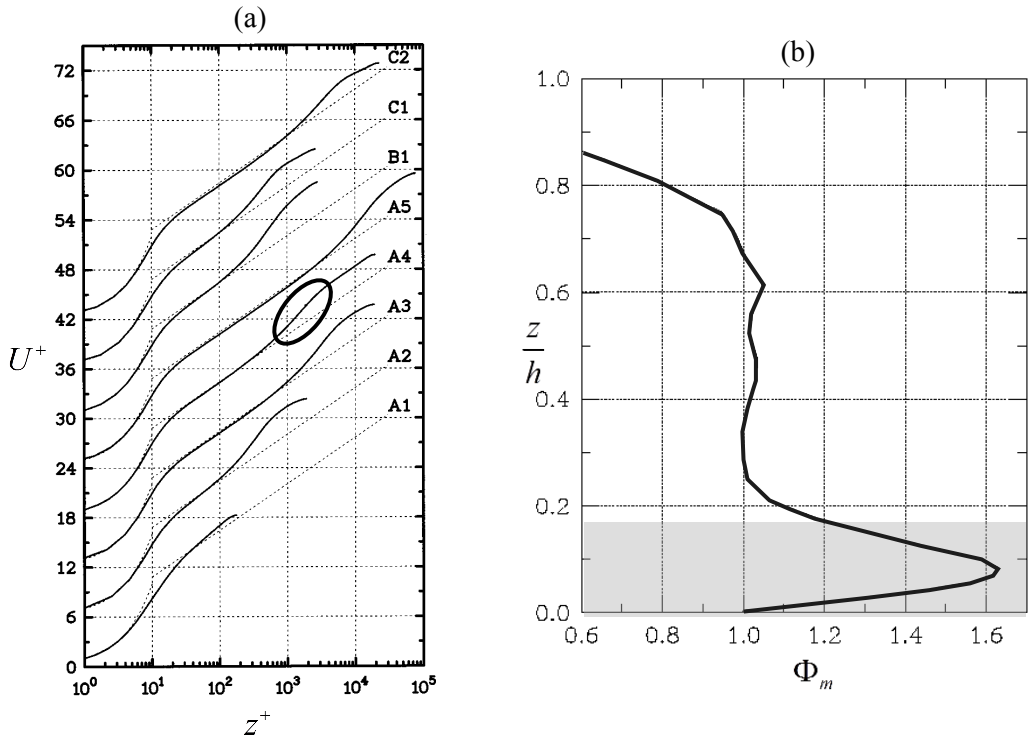

FIG. 2. The "logarithmic layer mismatch" in the smooth-wall turbulent channel flow detached-eddy simulations of Nikitin *et al.*[14], discussed by Spalart[15]. Curve A4 is the simulation in (b); $\mathrm{Re}_\tau = 20,000$. (a) $U^+ = U/u^*$ plotted against $z^+ = z/\ell_\nu$. (b) The "log layer mismatch" shown by the upper oval in (a) is shown here to be an overshoot in normalized mean shear Φ_m, negating LOTW scaling over the surface layer. Figure (b) was kindly generated by Spalart (private communication). κ is assumed to be 0.4.

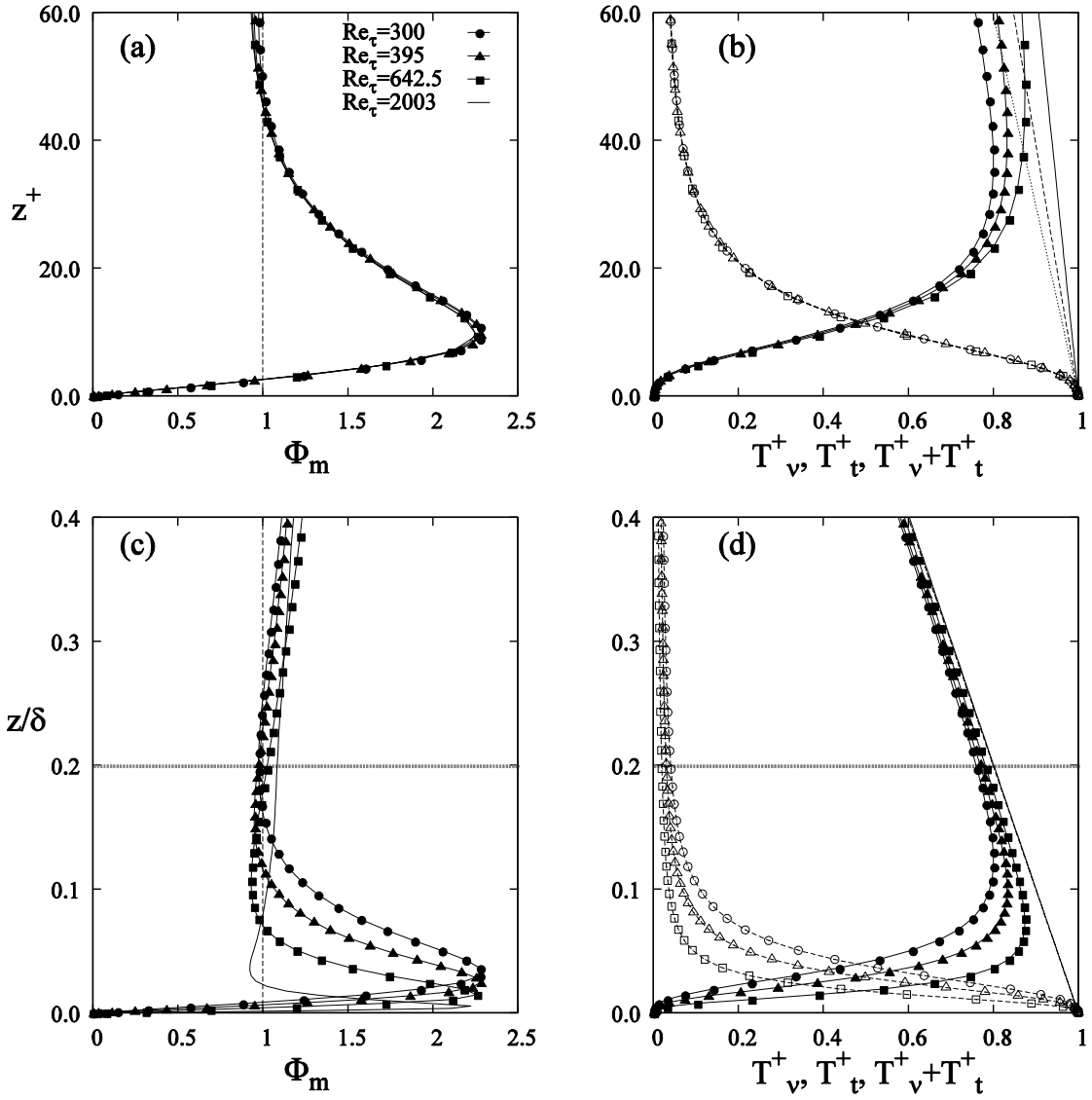

FIG. 3. DNS of the smooth-wall channel flow showing the physically real overshoot in the viscous region. (a) Normalized mean shear Φ_m vs. z^+. (b) Wall-normalized Reynolds shear stress T_t^+ (filled symbols) and mean viscous shear stress, T_ν^+ (open symbols) vs. z^+. The dotted, dashed and thin straight lines are the total shear stress profiles for Reynolds number of 300, 395, and 642, respectively. (c) Φ_m vs. z/δ, where δ is the half-channel height. (d) T_t^+ (filled symbols) and T_ν^+ (open symbols) vs. z/δ. Total shear stress profiles for three different Reynolds number collapse on to a single linear line. κ = 0.4 is assumed in forming Φ_m. Re_τ = 300, 395 and 642 DNS data are from Iwamoto *et al.*[34] and Iwamoto[35]; In (c) we have added the Re_τ = 2003 DNS data from Hoyas & Jimenez[36]. The horizontal dashed lines in (c) and (d) indicated the upper margin of the surface layer where LOTW should be predicted.

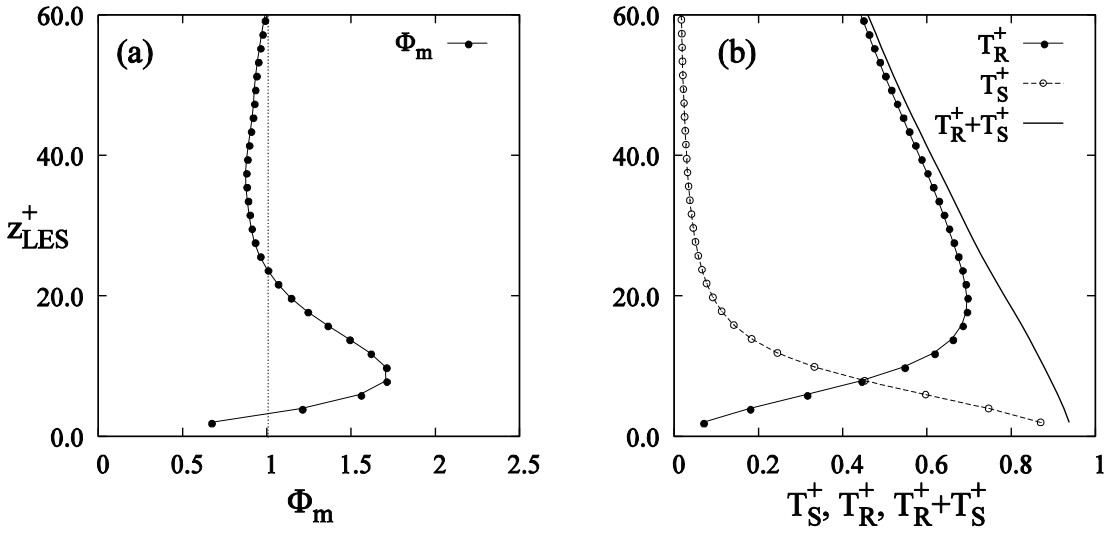

FIG. 4. Overshoot in LES of the neutral ABL using the Smagorinsky model ($C_s = 0.2$) and a $128 \times 128 \times 128$ grid. (a) Φ_m, vs. z^+_{LES}. (b) Wall normalized mean resolved and SFS shear stress, T_R^+, and T_S^+ plotted against z^+_{LES}, and its sum. κ = 0.4 is assumed in forming Φ_m. κ = 0.4 is assumed in forming Φ_m.

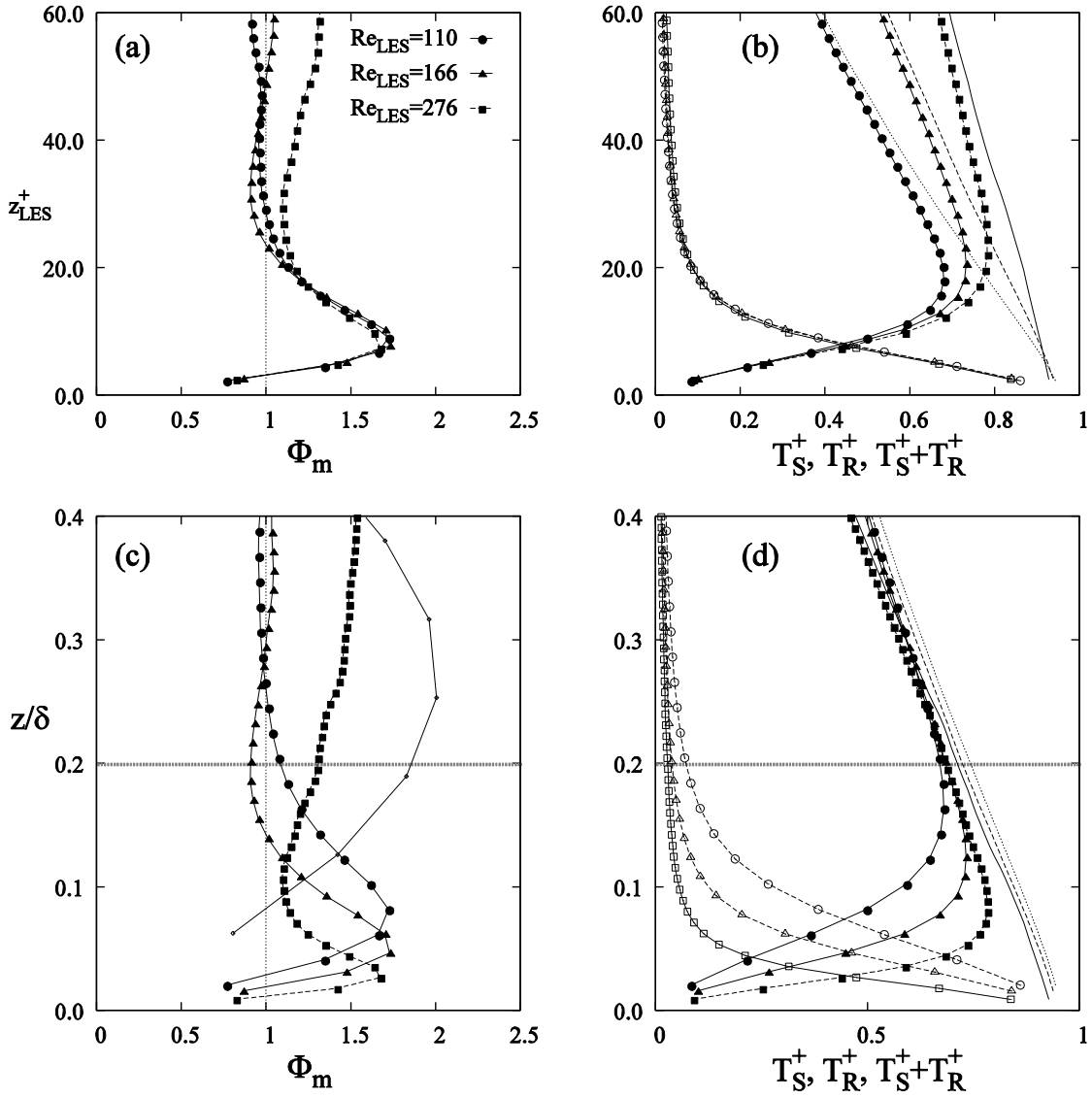

FIG. 5. Overshoots in LES of the neutral ABL. (a) Φ_m vs. z^+_{LES}. (b) Normalized resolved Reynolds stress T_R^+ (filled symbols) and mean SFS shear stress T_S^+ (open symbols) vs. z^+_{LES}. Dotted, dashed and thin lines are the sum of resolved and SFS stress, from low to high LES Reynolds number. (c) Φ_m vs. z/δ, where δ is defined as the height where $\Phi_m = 0$. (d) T_R^+ (filled symbols) and T_S^+ (open symbols) vs. z/δ. The LES Reynolds numbers of the simulations are shown in (a). In order of Re_{LES}, the Smagorinsky constants and grids were: ($C_s = 0.1, 42\times42\times96$), ($C_s = 0.2, 192\times192\times128$), and ($C_s = 0.1, 128\times128\times256$). The thin black line in (c) is a simulation with such low Re_{LES} that turbulence is barely sustained ($C_s = 0.2, 42\times42\times32$ and $\mathrm{Re}_{LES} = 38.$). The horizontal dashed lines in (c) and (d) indicated the upper margin of the surface layer where LOTW should be predicted. κ = 0.4 is assumed in forming Φ_m.

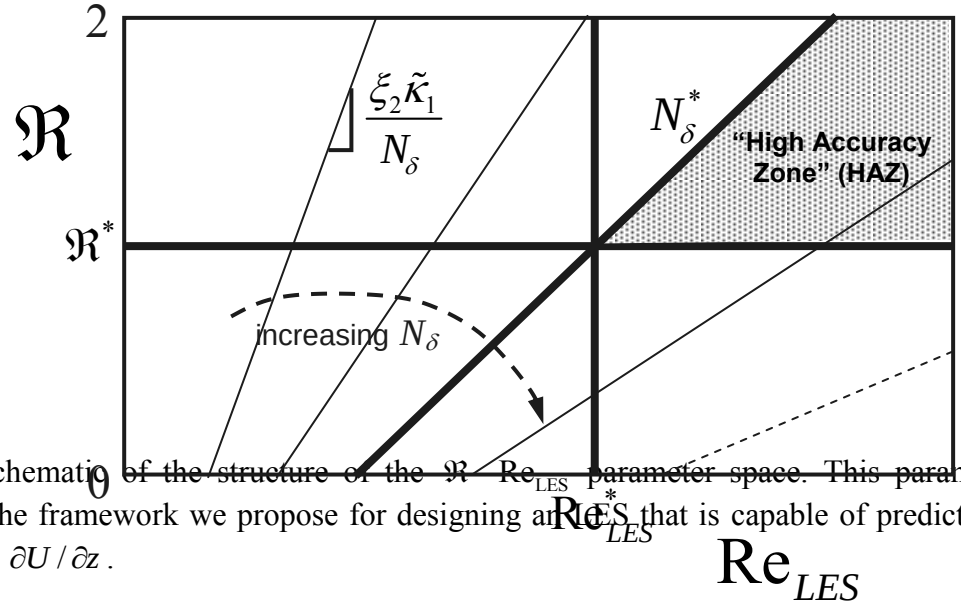

FIG. 6. Schematic of the structure of the $\Re - \mathrm{Re}_{\mathrm{LES}}$ parameter space. This parameter space underlies the framework we propose for designing an LES that is capable of predicting LOTW scaling for $\partial U / \partial z$.

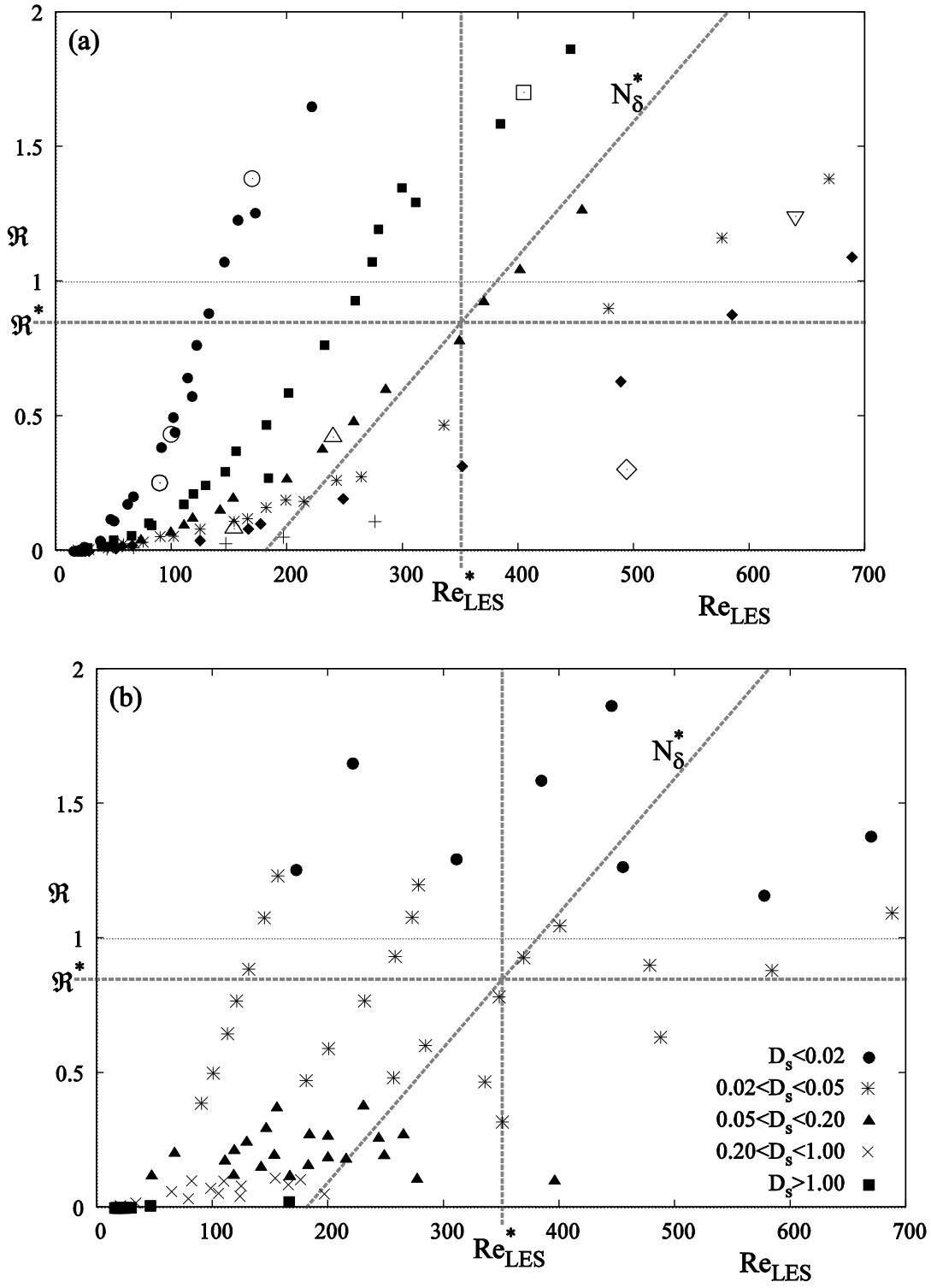

FIG. 7. The simulations carried out for this study shown on the $\Re - \mathrm{Re}_{\mathrm{LES}}$ parameter space. (a) The LES grouped according to N_z, where N_z = 32(●), 64(■), 96(▲), 128(✳), 160(◆) and 256(+). Also included are LES from several previous studies by Andren *et al.* 1994 (○), Sullivan *et al.*11 (Δ), Porté-Agel *et al.*[25] (□), Chow *et al.* 2005 [27] (◊) and Drobinski *et al.*[32] (▽). (b) The LES grouped according to $D_s = C_s^2 \mathrm{A_R}^{4/3}$.

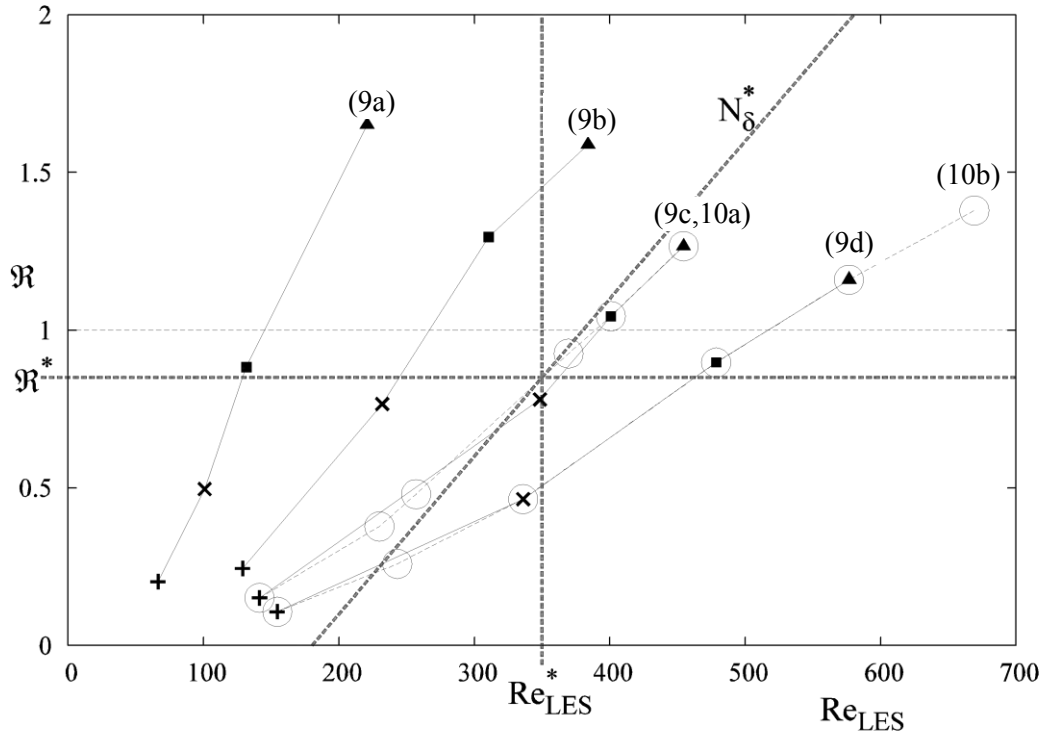

FIG. 8. The systematic variations on the $\Re - \mathrm{Re}_{LES}$ parameter space for the simulations plotted in Figs. 9 and 10. Fig. 9(a) shows four simulations with the same vertical resolution, $N_z = 32$, but decreasing $C_s^2 \mathrm{A_R}^{4/3}$ represented by +, ×, ■, ▲. The vertical resolutions in Figs. 9(b,c,d) are $N_z = 64$, 96, 128, respectively. The open circles show the locations of the 6 simulations in Figs. 9(a,b). The vertical resolutions in Figs. 10(a,b) are $N_z = 96$, 128, respectively.

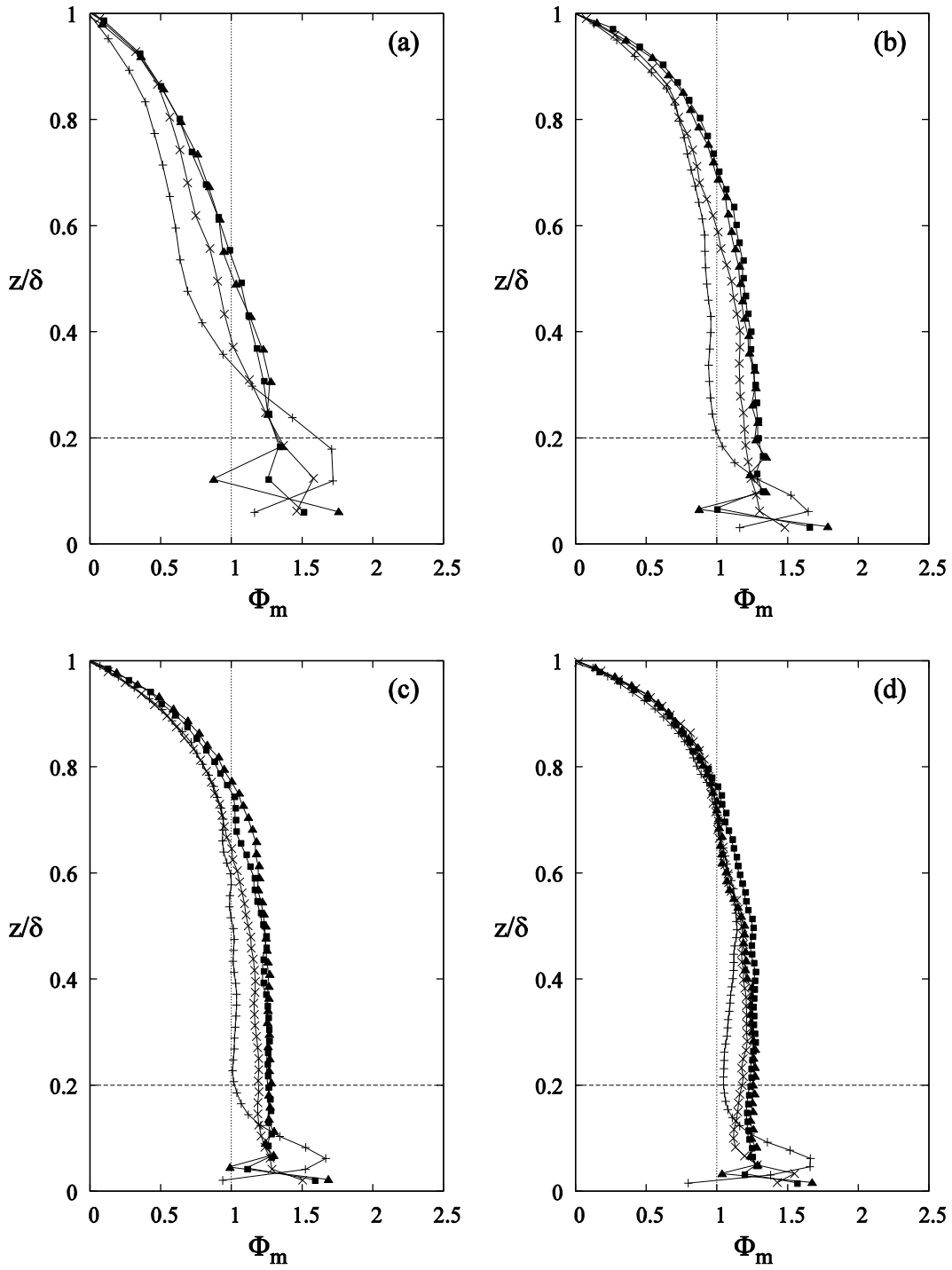

FIG. 9. Effect of vertical grid resolution on the LES predictions of mean shear. Refer to Fig. 8 for the locations of the individual simulations on the $\Re - \mathrm{Re}_{LES}$ parameter space. $\Re$ and Re_{LES} progressively increase in each figure in this order: +, ×, ■, ▲. (a) $N_z = 32$, $N_x = N_y$ increased from 32(+) to 128(▲). (b) $N_z = 64$, $N_x = N_y$ increased from 64(+) to 240(▲). (c) $N_z = 96$, $N_x = N_y$ increased from 64(+) to 288(▲). (d) $N_z = 128$, $N_x = N_y$ increased from 64(+) to 360(▲). κ = 0.4 is assumed in forming Φ_m. δ is defined as the height where $\Phi_m = 0$. The dashed horizontal lines indicated the upper margin of the surface layer.

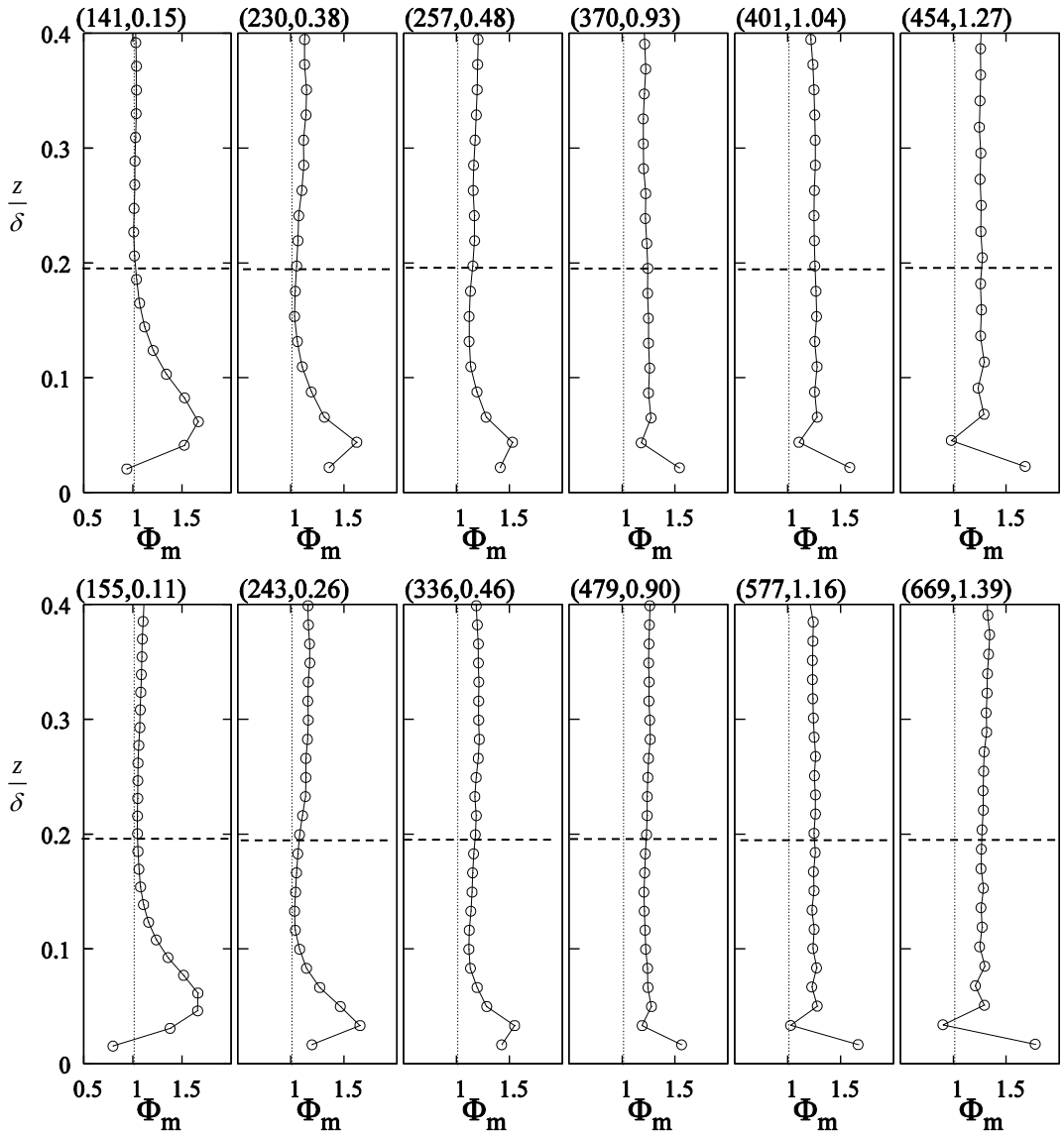

FIG. 10. Change of structure of $\Phi_m(z)$ as the LES move towards and into the HAZ. Refer to Fig. 8 for the locations of the individual simulations on the $\Re - \mathrm{Re}_{LES}$ parameter space; $\Re$ and Re_{LES} progressively increase in each panel from left to right. Top panel: LES with $N_z = 96$. Bottom panel: LES with $N_z = 128$. Re_{LES} and $\Re$ are given on top of each figure, as (Re_{LES}, $\Re$). $\kappa = 0.4$ is assumed in forming Φ_m. δ is defined as the height where $\Phi_m = 0$. The horizontal dashed lines indicate roughly the upper-most margin of the surface layer.

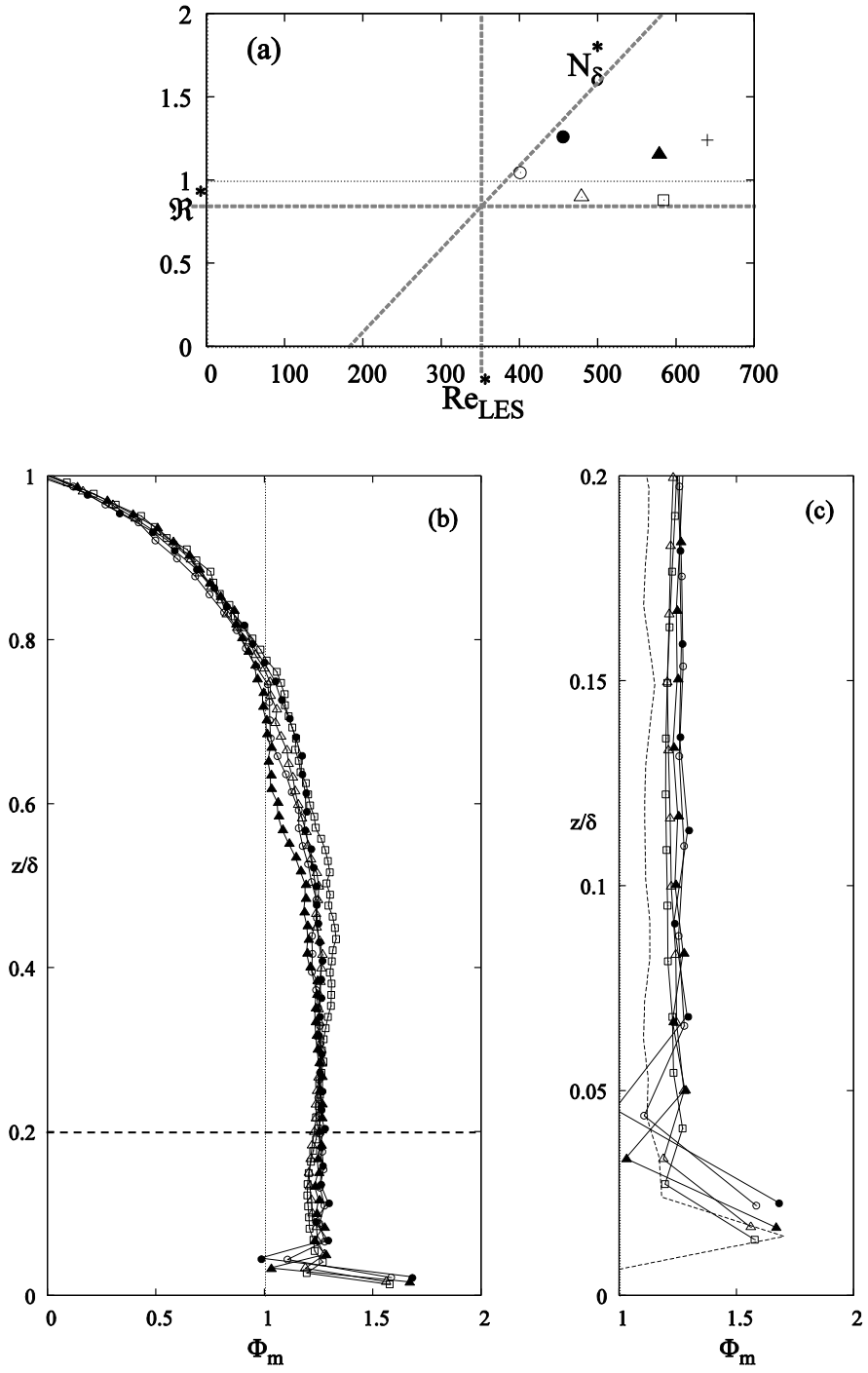

FIG. 11. Five simulations in the HAZ at different N_δ and $D_s \equiv C_s^2 A_R^{4/3}$, demonstrating the convergence of the predictions of $\Phi_m(z)$ to a relatively grid-independent solution without the overshoot and capturing the LOTW. Figure (a) gives the locations of the 5 simulations in HAZ. $\Phi_m(z)$ from Drobinski *et al.*[32] are given in (c) with the dashed curve and in (a) with the plus symbol (+). $\kappa = 0.4$ is assumed in forming Φ_m. δ is defined as the height where $\Phi_m = 0$.